UNIVERSITY OF GAZİANTEP

GRADUATE SCHOOL OF

NATURAL&APPLIED SCIENCES

CALCULATION OF STOPPING POWER FOR POSITRONS THROUGH MATTER

M.Sc THESIS

IN

ENGINEERING OF PHYSICS

BY

FATİH ETOĞLU

AUGUST 2012

Calculation of Stopping Power for Positrons Through Matter

M.Sc Thesis
in
Engineering of Physics
University of Gaziantep

Supervisor
Prof.Dr. Zihni ÖZTÜRK

by
Fatih ETOĞLU
August 2012

REPUBLIC OF TURKEY
UNIVERSITY OF GAZİANTEP
GRADUATE SCHOOL OF NATURAL & APPLIED SCIENCES
DEPARTMENT OF ENGINEERING PHYSICS

Name of thesis : Calculation of Stopping Power for Positrons Through Matter.

Name & Surname of Student: Fatih ETOĞLU

Exam date : 23.08.2012

Approval of the Graduate School of Natural Science and Applied Science

Prof. Dr. Ramazan KOÇ
Director

I certify that this thesis satisfies all the requirements as a thesis for degree of Master of science.

Prof. Dr. A.Necmeddin YAZICI
Head of Department

This is to certify that we have read this thesis and that in our consensus/majority opinion it is fully adequate, in scope and quality, as a thesis for degree of Master of Science.

Prof. Dr. Zihni ÖZTÜRK
Supervisor

Examining Committee Members	Signature
Prof. Dr. Zihni ÖZTÜRK	.....
Y.Doç.Dr.Güler YILDIRIM	.....
Y.Doç.Dr.Serap ÇELİK	.....

I hereby declare that all information in this document has been obtained and presented in accordance with academic rules and ethical conduct. I also declare that, as required by these rules and conduct, I have fully cited and referenced all material and results that are not original to this work.

Fatih ETOĞLU

ABSTRACT

CALCULATION OF STOPPING POWER FOR POSITRON THROUGH MATTER

ETOĞLU, FATİH
M.SC. in Engineering of Physics
Supevisor: Prof. Dr. Zihni ÖZTÜRK
August 2012
52 pages

In this work, the stopping power of the positron in Al, Si, Ag, Cu, and Pb elements were calculated by using five different formulations. Some of these formulations are theoretical and some of them are emprical. It is difficult to obtain the exact result of stopping power for the positrons. Therefore, many attempts have been done by the researchers to obtain empirical formulations and to estimate the stopping powers of the positron in the elements. It was found that each method provides a proper result depending on the the energy range of the positron.

Stopping power of the positron have a wide application in radiation dosimetry. The knowledge of the ranges and stopping powers of this particle in matter has useful applications for the study of biological effects, radiation damage dosage-rates and energy dissipation at various depths of an absorber. It has also useful applications in the design of detection systems, radiation technology, semi-conductor detectors, shielding and choosing the proper thickness of the target.

Keywords: Positron, Stopping power, Pet,Interaction of charged particles

ÖZ

MADDE İÇERİSİNDE POZİTRONUN DURDURMA GÜCÜNÜN HESAPLANMASI

ETOĞLU, FATİH
Yüksek Lisans Tezi, Fizik Mühendisliği Bölümü
Tez Yöneticisi: Prof. Dr. Zihni ÖZTÜRK
Ağustos 2012
52 sayfa

Bu çalışmada, beş farklı formül kullanılarak, pozitronun , Al, Si, Ag, Cu, ve Pb elementleri içinde durdurma gücü hesaplandı. Bu formüllerin bazıları teorik, bazıları ise deneyseldir. Pozitronun durdurma gücü için, kesin bir sonuç elde etmek zordur. Bundan dolayı, elemenlerin içinde, deneysel formüller elde etmek için ve pozitronun durdurma gücünü tahmin etmek için, birçok araştırmacı tarafından girişimlerde bulunulmuştur. Şu tesbit edilmiştir ki, her metod, uygun sonucu pozitronun enerji aralığına bağlı olarak vermektedir.

Pozitronun durdurma gücünün, radyasyon dozimetrisinde, geniş bir uygulama alanı vardır. Bu taneciğin madde içindeki menzili ve durdurma gücünün bilinmesinin uygulama alanları vardır. Bunlar; biyolojik etkiler, radyasyonun zararı-doz oranları ve bir malzemenin çeşitli derinliklerdeki enerji kaybıdır. Ayrıca tespit sistemlerinin dizaynında, radyasyon teknolojisinde, yarı iletken dedektörlerde, korunmada ve hedef malzemenin uygun kalınlığını seçiminde de, pozitronun durdurma gücünden faydalanılır.

Anahtar Kelimeler: Pozitron, Durdurma gücü, Pet,Yüklü taneciklerin etkileşimi

ACKNOWLEDGEMENT

I would like to thank my supervisor Prof. Dr. Zihni ÖZTÜRK for his helps and advice during this study and to my wife Özgül ETOĞLU for her patience and helps also I would like to thank other personnel at the department of Engineering Physics for their kindness and friendships.

TABLE OF CONTENTS

LIST OF FIGURES

LIST OF TABLES

CHAPTER 1

INTRODUCTION

In this work, the stopping power of the positron in Al, Si, Ag, Cu, and Pb elements were determined by using different methods. It is difficult to obtain the exact result of stopping power for the positrons. Hence many attempts have been done by the researchers to obtain empirical formulations to calculate the stopping powers of the positron in the matters. It was found that each method provides a proper result depending on the the energy range of the positron

According to the Bethe formula, many attempts have been done by the researchers to obtain empirical formulations to estimate the stopping powers of the positron in the elements.

- Batra and Sehgal, 1970;
- Gupta et al, 1982;
- Tsoulfanidis, 1995;
- Rohrlich and Carlson, 2005;
- P.B.Pal et al, 2008.

Every formula is used for different energy levels. We tried to find out which formula gives the proper results according to the energy value of the positron and the material.

P. Dirac printed a paper explaining that electrons have both negative energy and a positive charge in 1928 [1]. To explain the Zeeman effect, Dirac equation presented a unification of quantum mechanics, special relativity, and also new description of electron spin. As a result, the work didn't find a new particle clearly, but proved that an electron can have either positive or negative energy. With experimental results, he provides the positive-energy explanation. But Dirac doubted

by the equally valid negative-energy solution that the mathematical model allowed. Quantum mechanics did not allow the negative energy solution to simply be ignored, as classical mechanics often did in such equations; the dual solution showed the possibility of an electron spontaneously jumping between positive and negative energy states. But, no such transition had yet been obtained experimentally. He carried to the issues raised by this conflict between theory and observation as "difficulties" that were "unresolved".

In December 1929 Dirac wrote a paper again [2]. that tried to explain the unavoidable negative-energy solution for the relativistic electron. He declared that "an electron with negative energy moves in an external electromagnetic field as though it carries a positive charge." He further adduced that all of space could be thought as a "sea" of negative energy states that were filled, so as to prevent electrons jumping between positive energy states (negative electric charge) and negative energy states (positive charge). The paper also explained the possibility of the proton being an island in this sea, and that it may actually be a negative-energy electron. Dirac accepted that the proton having a much greater mass than the electron was a problem, but expressed "hope" that a future theory would resolve this issue.

Robert Oppenheimer denied to Dirac's equation that the proton can not be the negative-energy electron solution [3]. He declared that if it were, the hydrogen atom would rapidly self-destruct. Persuaded by Oppenheimer's argument, Dirac published a paper in 1931 that predicted the existence of an as-yet unobserved particle that he called an "anti-electron" that would have the same mass as an electron and that would mutually annihilate upon contact with an electron [4].

1.1 Discovery and Experimental Clues

First Dmitri Skobeltsyn detected the positron in 1929 by using a Wilson cloud chamber to try to find gamma radiation in cosmic rays, Skobeltsyn detected particles that acted like electrons but curved in the opposite direction in an applied magnetic field [5].

Likewise, in 1929 Chung-Yao Chao, a graduate student at Caltech, discovered some extraordinary outcomes that indicated particles acting like

electrons, but with a positive charge, though the outcomes were indefinite and the phenomenon was not pursued [6].

The positron was found by Carl D. Anderson on August 2, 1932. For this reason in 1936 he won the Nobel Prize for Physics [7]. And also Anderson invented the term positron. The positron was the first proof of antimatter or antiparticle and was discovered when Anderson allowed cosmic rays to pass through a cloud chamber and a lead plate. A magnet covered this equipment, resulting particles to curve in different directions depending on their electric charge. The ion trail left by each positron appeared on the photographic plate with a curvature matching the mass-to-charge ratio of an electron, but in a direction that showed its charge was positive.

Anderson thought in looking back that the positron would have been invented earlier with Chung-Yao Chao's work, if only it had been put through. The Joliot-Curies in Paris had proof of positrons in old photographs when Anderson's results show up but they had misunderstood them as protons.

1.2 Positron Decay (Beta Decay)

A positron is a positively charged electron. It's an antielectron or antimatter. The positron has a charge of +1 (just the opposite of the -1 of the electron), and a spin of 1/2 as an electron does. The mass of this elementary particle is about 9.103826×10^{-31} kg. The actual charge on this particle is about $+1.602 \times 10^{-19}$ coulombs. It can be written as β^+ or e^+ in nuclear equations.

$$p \rightarrow n + e^+ + \upsilon_e$$

In an atomic nuclei which has excess protons, a proton can be converted to a neutron, a positron and an electron type neutrino .

$$e^- + e^+ \rightarrow 2\gamma$$

When a low energy positron collide with a low energy electron an annihilation occurs and two or more gamma rays occurs

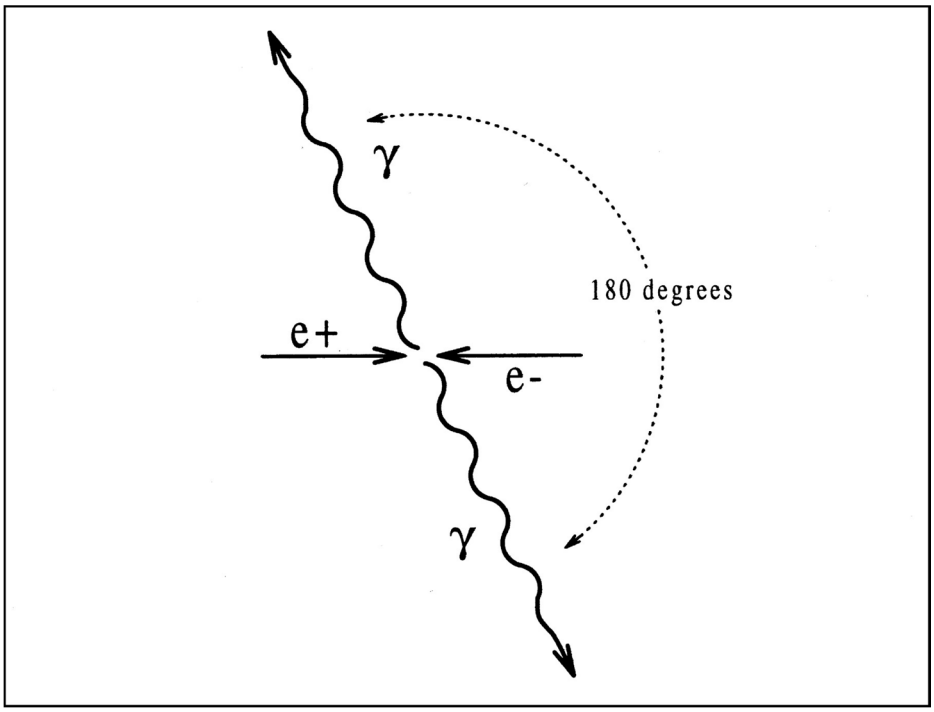

Figure 1.1 The occurance of annihilation radiation

1.3 Definition of Stopping power

Stopping power is described as the average energy loss of the charged particles due to ionizations and excitations as well as the radiation loss.

In radiation dosimetry, positron stopping power have a broad application. But, having an accurate value for the stopping power of positron is so difficult.

1.4 Stopping Power

To understand the interaction mechanism, with matter, the total stopping power of electron and positron is an useful way. In nature, mathematical formula for the total stopping power is complex. Average stopping power for electrons and positrons in matter from these mathematical formulas is complicated and needs use of mean excitation and ionization energies. Many empirical studies have been done about total stopping power of materials during the last decades. Nuclear physics scientists can compute stopping power of positron, continuous slowing down approximation (csda) ranges and other effects very clearly. The simple formula for the stopping power of electrons and positrons in different materials are usually used in many useful areas in nuclear spectroscopy, radiation dosimetery, surface layer

analysis, physics of organic scintillators and semiconductor detectors. The total stopping power of electrons and positrons is described as the average energy loss per unit path length because of the ionization and excitation losses. Many researchers have formed the theory of collision loss of electrons and positrons depending on the material properties and energy parameters to evaluate the collision stopping power of electron and positron and found theoretical and emprical formulas for calculating the radiation loss of positron [Batra and Sehgal, 1970; Gupta et al, 1982; Tsoulfanidis, 1995; Rohrlich and Carlson, 2005; P.B.Pal et al, 2008],

There have been some important new ideas in these extents. These progresses depend heavily on new advance in empirical methods, and to a larger areas on the insights gained through close working between theorists and experimentalists doing research on physical properties of solids. Empirical terms such as valence electron, ionic charge, atomic number, electro negativity and energy are then effective. These terms are directly related with the character of the chemical bond and so give ideas for explaining and classifying many basic properties of molecules and solids. In many cases empirical relations do not give highly accurate results for each specific material, but they still can be very useful.

Particularly, the simplicity of empirical formulations provides a larger class of researchers to evaulate usable properties, and often trends become more evident. In the modified proposed empirical relation just the atomic number, density and total energy of electrons and positrons are used as input parameters, thus the evaulation of the stopping power becomes trivial; and the results reveals are comparable to the experimental and theoretical values.

The knowledge of the features of the transmission and absorption of low, intermediate and high energy positron in elemental materials is of great importance for the experimental methods in nuclear and atomic physics. It is also useful in understanding the various interactions of these particles with matter.

The knowledge of the ranges of this particle in matter has useful applications for the study of biological effects, radiation damage dosage-rates and energy dissipation at various depths of an absorber. It has also useful applications in the design of detection systems, radiation technology, semi-conductor detectors and shielding by choosing the proper thickness of the target.

Many experimentals as well as the theoretical studies have been made with the object of establishing standard range-energy relations.

Easy empirical formulas are very helpful in the study of energy straggling, target foil thickness estimation and in particle identification studies. The important aspect of such problem is to know the energy loss incurred by the charged particle during the course of their passage in the absorber.

1.5 Energy loss of Light Charged Particles with Matter

Electrons and positrons are light charged particles (or beta particles). It will be examined that how light charged particles interact in material and working on their behavior with comparing heavy charged particles relation with mechanisms of energy loss, track, range. It will be seen that the very big difference in mass between the heavy and light charged particles has important consequences for interactions.

1.6 Interaction of Electron (Beta Interaction)

A beta particle jumps from the nuclide of an atom, Because of this, it is called beta particle. The energy of the beta particle is proportional with the velocity, and inversely, since it has small mass, its energy with MeV range. When an energetic electron (beta) passes over matter, it interacts with material through Coulomb interactions with atomic orbital electrons and atomic nucleus. When the electrons leave the interaction site, they immediately start to transfer their energy to the surrounding material, as shown in Figure 1.2. Electrons can interact with the other electrons without touching. Because they carry electrical charge. As an electron passes over to the material, it forces the other electrons away from its path. As the enough energy is given to the other electron to eject from the atom, ionization occurs.

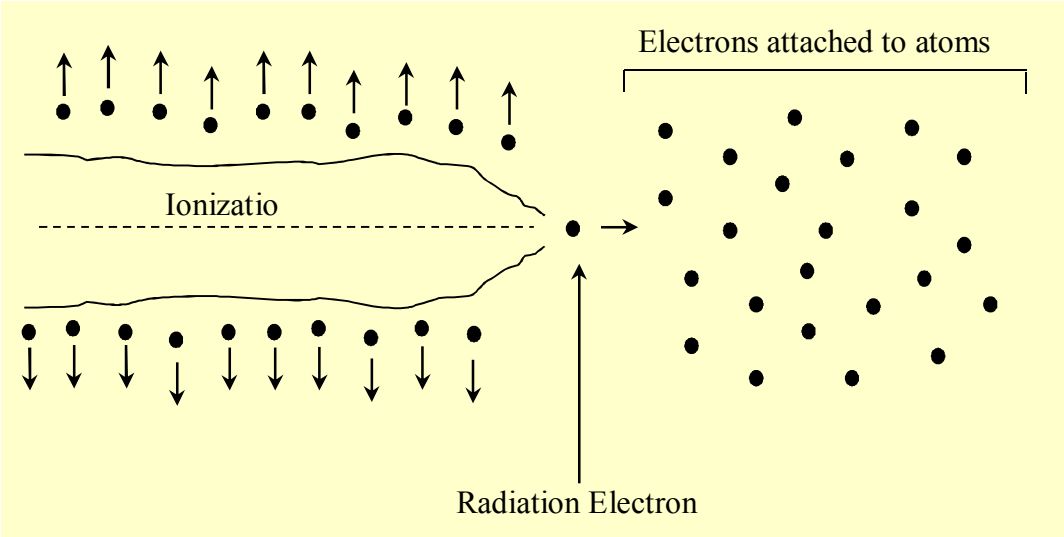

Figure 1.2 Ionization produced by a radiation electron

In general, before an electron spends the whole energy, it makes a lot of interactions. Due to these collisions (elastic or inelastic scattering) the electrons lose the kinetic energy with collision or radiative losses or both of them. Thus, energy is transferred to the medium or changes their direction of travel (scattering). So, beta particles can transfer the energy to a medium in four ways: direct ionization, delta rays, bremsstrahlung radiation, and Cerenkov radiation. Each interaction can occur, but ionization and bremsstrahlung are the most important interactions.

Stopping power describes the energy losses; scattering power describes the scattering. Stopping power is the term used to express the gradual energy loss of the charged particle when it interacts with an absorbing material. There are two types of stopping powers: Collision (ionization) stopping power that causes by interaction of the charged particle with orbital electrons of the atom and radiative stopping power (bremsstrahlung) that causes by interaction of the charged particle with nucleus of the atom. Excitations and ionizations occur with columbic interaction between the orbital electrons of the atom and incident electron. Ionizations and excitations occur in collisional energy losses and are named with collision (ionization) stopping powers. Columbic interactions of the incident electron with nuclei of the absorber atom result in electron scattering and energy loss of the electron through production of X-ray photons which is labeled as bremsstrahlung. These energy losses are called as radiative stopping powers of positron.

1.7 Kerma (Kinetic energy released in material)

KERMA is used to express the energy loss in a matter. It is a unit of exposure that describes the kinetic energy transferred to charged particles per unit mass of irradiated medium when indirectly ionizing (uncharged) radiations such as photons or neutrons traverse the medium. Kerma is thus the starting point to determine the energy deposition by a given type of radiation in an absorbing medium and changes with radiation type and absorption medium.

There are two types of collisions between the incident electron and orbital electron or nuclei of the radioactive atom. These are elastic and inelastic collisions. In an elastic collision the electron is scattered from its original path but results no energy loss. However, in an inelastic collision, the electron is scattered from its original path and it gives some of its energy to an orbital electron or as bremsstrahlung. Characteristic X-rays will also be emitted as these vacancies are filled if the beta particles eject K, L, or M shell electrons. As energetic electrons traverse an absorber they make thousands of collisions, thus their behavior is described by a statistical theory of multiple scattering embracing the individual elastic and inelastic collisions with orbital electrons and nuclei.

The type of interaction that the electron undergoes with a particular atom of radius *a* depends on the impact parameter *b* of the interaction, defined as the perpendicular distance between the electron direction before the interaction and the atomic nucleus (see Figure 1.3).

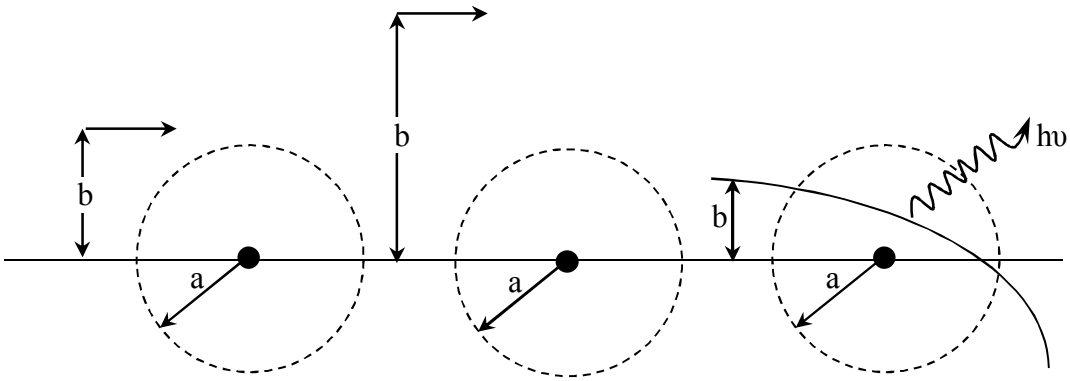

Figure 1.3 Interaction of an electron with an atom, where a is the atomic radius and b is the impact parameter.

If *b* is larger than *a*, the electron makes a soft collision with the all atom and only a small amount of energy is transferred from the incident electron to orbital electrons of the atom.

If *b* is almost equal to *a*, the electron makes a hard collision with an orbital electron of the atom and lots of energy of the incident electron is transferred to the orbital electron.

If *b* is smaller than *a*, the incident electron makes a radiative interaction (bremsstrahlung) with the atomic nuclei. The electron emits a photon with energy between zero and the kinetic energy of the incident electron the magnitude of the impact parameter *b* determines the emitted photon bremsstrahlung energy. The energy of the bremsstrahlung photon is inversely proportional with the impact parameter. The yield or fraction of bremsstrahlung produced is proportional to the atomic number of the target (or absorbing) material and the energy of the electrons striking the target, which of course rapidly decreases as the particles traverse the target material. The deflecting force is directly proportional to the nuclear charge (or *Z*) of the target. As charged particles are absorbed in matter (which has a low atomic number), less than 1% of the interactions cause bremsstrahlung, and lots of them that do are likely to run away the medium because their probability of interaction is also low in this low-*Z* medium. High-speed charged particles may result the emission of visible radiation with a blue tint which is named Cerenkov radiation.

1.8 Types of Energy Losses

1.8.1 Collision Losses:

An electron losses its energy due to interactions with orbital electrons in the medium, like heavy charged particles. This results excitation of the atom (an orbital electron go to a higher energy shell) or ionization (to overcome its binding energy to the atom, enough energy is transfered to the electron and it escapes the atom altogether). This type of energy loss is named collisional loss. Because electrical forces effect over long distances, in fact, the collision between the two charged particles may occur without touching each other.

By looking the behavior of heavy charged particles, the maximum energy transfer occurs in a “head-on” collision between two particles of masses *m* and *M*

$$Q_{max} = \frac{4mME}{(M+m)^2} \tag{1.1}$$

Where E is the kinetic energy of the incident particle. For light charged particles, $m = M$ and $Q_{max} = E$. So, In a single collision, the maximum energy transferred is all of it. Obviously this view of electron behavior is importantly different from the behavior of heavy charged particles. Mass is the second important difference in behaviour between light charged particles and heavy charged particles. A particle interacting with a particle of the same mass and thus a very large scattering angles are possible. This result in a path that is very complicated comparing to the direct path of a alpha particle or proton.

1.8.2 Radiative Losses

Another important difference between light and heavy particles is the small mass of the light charged particle. Thus, there is an second energy loss mechanism.

A charged particle makes a change in acceleration always gives electromagnetic radiation. This electromagnetic radiation is named as bremsstrahlung. The more energetic the photon, the larger the change in acceleration. A heavy charged particle, while going away by a charged nucleus, makes little deflection in its trace. But, an electron may be deflected strongly, due to the little mass. Because of this, it can be obtained that important bremsstrahlung with electrons interacting in matter, and unimportant bremsstrahlung with heavy particles. The deflection is very large and the emitted photon is very energetic if the electron passes close to the nucleus,. But, the emitte d photon will be less energetic if the electron passes far from the nucleus. So, the bremsstrahlung photons show a continuous energy dispersion that ranges downward from a maximum equal to the kinetic energy of the incoming electron.

In this context, for light charged particles, the total stopping power is equal to the sum of both collisional and radiative stopping powers.

$$\left(-\frac{dE}{dx}\right)^{\pm}_{tot} = \left(-\frac{dE}{dx}\right)^{\pm}_{coll} + \left(-\frac{dE}{dx}\right)^{\pm}_{rad} \tag{1.2}$$

Though collisional energy loss, there is no simple mathematical formulation to calculate the bremsstrahlung energy loss (called as radiative energy loss) On the

other hand, it is much easier to measure. Radiation energy loss is quite different from collisional energy loss. The effectiveness of bremsstrahlung in matter of different atomic number Z changes closely as Z^2. Therefore, for beta particles of a given energy, in high-Z materials bremsstrahlung losses are significantly larger (e. g. lead) than in low-Z materials (e. g. water). In an element, the collisional energy loss is directly proportional to n and so to Z and also, the radiative energy loss rate increases just logarithmically. Thus, for beta particles bremsstrahlung becomes the predominant interaction mechanism of energy loss, at high energies as shown in Table 1.1

Above close formula can be used, to obtain the the ratio of radiative and collisional stopping powers for an electron of total energy E, described in MeV, in an element of atomic number Z

$$\frac{\left(-\frac{dE}{dx}\right)_{rad}^{-}}{\left(-\frac{dE}{dx}\right)_{coll}^{-}} \cong \frac{ZE}{800} \tag{1.3}$$

This formula gives that for example in lead (Z=82), the two rates of energy loss are nearly equal at a total energy given by

$$\frac{82E}{800} \cong 1 \tag{1.4}$$

So, $E \cong 9.8\ MeV$, and the kinetic energy of the electron is $T = E - mc^2 \cong 9.3$ MeV. In oxygen (Z = 8), the two rates are equal as $E \cong 100\ MeV \cong T$.

The dominance of radiative over collisional energy losses shows rise to electron-photon cascade showers at very high energies. Because the bremsstrahlung photon spectrum is nearly flat out to its maximum (equal to the kinetic energy of the electron), beta particles with high energy result high-energy photons. These, in turn, generate positron-electron pairs and compton electrons, in this way it generates more bremsstrahlung photons, and so on. These type interactions produce an electron-photon cascade shower, which can be started by either a photon or a high-energy beta particle.

Additionaly, energy loss mechanism and collision characteristics of positron are almost identical to the electron behaviour.

Table 1.1 Electron Collisional, Radiative, and Total Mass Stopping Powers

Kinetic Energy	β^2	$\left(-\frac{1}{\rho}\cdot\frac{dE}{dx}\right)^{-}_{col}$ ***(MeV cm^2 g^{-1})***	$\left(-\frac{1}{\rho}\cdot\frac{dE}{dx}\right)^{-}_{rad}$ ***(MeV cm^2 g^{-1})***	$\left(-\frac{1}{\rho}\cdot\frac{dE}{dx}\right)^{-}_{tot}$ ***(MeV cm^2 g^{-1})***
10 **eV**	0.00004	4.0	-	4.0
30	0.00012	44.	-	44.
50	0.00020	170.	-	170.
75	0.00029	272.	-	272.
100	0.00039	314.	-	314.
200	0.00078	298.	-	298.
500 **eV**	0.00195	194.	-	194.
1 **keV**	0.00390	126.	-	126.
2	0.00778	77.5	-	77.5
5	0.00193	42.6	-	42.6
10	0.00380	23.2	-	23.2
25	0.0911	11.4	-	11.4
50	0.170	6.75	-	6.75
75	0.239	5.08	-	5.08
100	0.301	4.20	-	4.20
200	0.483	2.84	0.006	2.85
500	0.745	2.06	0.010	2.07
700 **keV**	0.822	1.94	0.013	1.95
1 **MeV**	0.886	1.87	0.017	1.89
4	0.987	1.91	0.065	1.98
7	0.991	1.93	0.084	2.02
10	0.998	2.00	0.183	2.18
100	0.999+	2.20	2.40	4.60
1000 **MeV**	0.999+	2.40	26.3	28.7

1.9 Positron Emission Tomography (PET)

PET expresses Positron Emission Tomography and it is used to determine the disease of the body. It is an imaging technique which uses small amounts of radiolabeled tracers. The tracers are biologically active compounds and they are

injected into the body, or it is got in with breathing of a gas, and then a PET scanner is used to have an image which shows the dispersion of the tracer in the body.

1.10 Discovery

Dr.Michael Phelps in 1973 first produces the “Brain Camera” at Washington University. In 1976, to set the world’s biggest PET program, Phelps went to UCLA.

He founded PET clinic at UCLA for patients. There are almost 800 clinics all over the world. Now, Michael Phelps is chairman at UCLA.

1.11 The physical principles of PET.

After injection of a tracer compound labeled with a positron emitting radionuclide the subject of a PET study is placed within the field of view (FOV) of a number of detectors capable of registering incident gamma rays. The radionuclide in the radiotracer decays and the resulting positrons subsequently annihilate on contact with electrons after travelling a short distance (~ 1 mm) within the body. Each annihilation produces two 511 keV photons travelling in opposite directions and these photons may be detected by the detectors surrounding the subject. The detector electronics are linked so that two detection events unambiguously occurring within a certain time window may be called coincident and thus be determined to have come from the same annihilation. These "coincidence events" can be stored in arrays corresponding to projections through the patient and reconstructed using standard tomographic techniques. The resulting images show the tracer distribution throughout the body of the subject. This section describes the physical principles underlying PET and discussing some of the intrinsic advantages that PET exhibits over Single Photon Emission Computed Tomography (SPECT) techniques.

1.12 Annihilation and Positron emission

Proton-rich isotopes may decay via positron emission, in which a proton in the nucleus decays to a neutron, a positron and a neutrino. The daughter isotope has an atomic number one less than the parent. Examples of isotopes which undergo decay via positron emission are shown in Table 1.2

Table 1.2 Properties of commonly used positron emitting radio-isotopes

Isotope	half-life(min)	Maximum positron energy (MeV)	Positron range in water(FWHM in mm)	Production method
^{11}C	20.3	0.96	1.1	cyclotron
^{13}N	9.97	1.19	1.4	cyclotron
^{15}O	2.03	1.70	1.5	cyclotron
^{18}F	109.8	0.64	1.0	cyclotron
^{68}Ga	67.8	1.89	1.7	generator
^{82}Rb	1.26	3.15	1.7	generator

As positrons travel through human tissue they give up their kinetic energy principally by Coulomb interactions with electrons. As the rest mass of the positron is the same as that of the electron, the positrons may undergo large deviations in direction with each Coulomb interaction, and they follow a tortuous path through the tissue as they give up their kinetic energy (Figure 1.4).

When the positrons reach thermal energies, they start to interact with electrons either by annihilation, which produces two 511 keV photons which are anti-parallel in the positron's frame, or by the formation of a hydrogen-like orbiting couple called positronium. In its ground-state, positronium has two forms - ortho-positronium, where the spins of the electron and positron are parallel, and para-positronium, where the spins are anti-parallel. Para-positronium again decays by self-annihilation, generating two anti-parallel 511 keV photons. Ortho-positronium self-annihilates by the emission of three photons (Evans, 1955) [8]. Both forms are susceptible to the pick-off process, where the positron annihilates with another electron. Free annihilation and the pick-off process are responsible for over 80% of the decay events. Variations in the momentum of the interacting particles involved in free annihilation and pick-off result in an angular uncertainty in the direction of the

511 keV photons of around 4 mrad in the observer's frame (Rickey et al 1992) [9]. In a PET camera of diameter 1m and active trans axial FOV of 0.6m this results in a positional inaccuracy of 2-3 mm.

The finite positron range and the non-collinearity of the annihilation photons give rise to an inherent positional inaccuracy not present in conventional single photon emission techniques. However, other characteristics of PET which are discussed below more than offset this disadvantage.

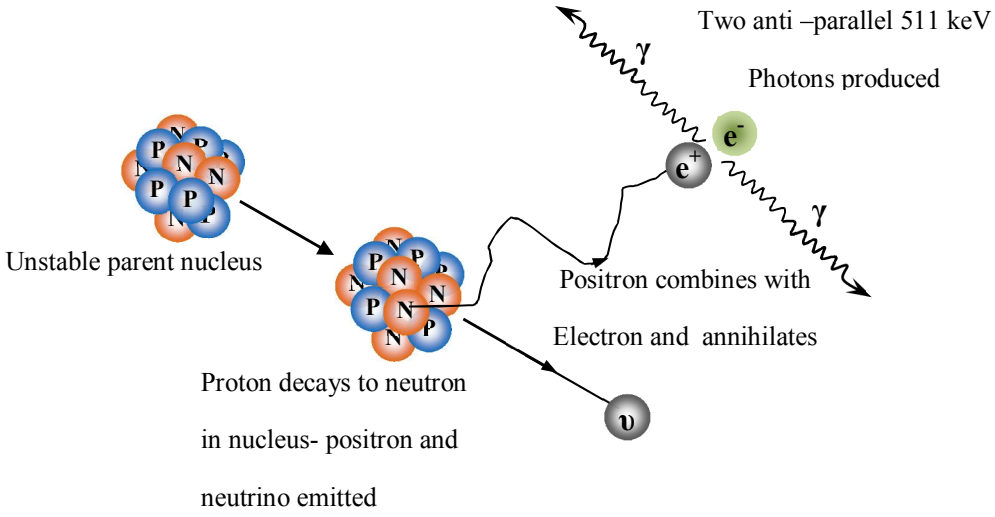

Figure 1.4 Positron emission and annihilation

1.13 Electronic collimation and coincidence detection

In a PET camera, each detector generates a timed pulse when it registers an incident photon. These pulses are then combined in coincidence circuitry, and if the pulses fall within a short time-window, they are deemed to be coincident. A conceptualized diagram of this process is shown in figure 1.5.

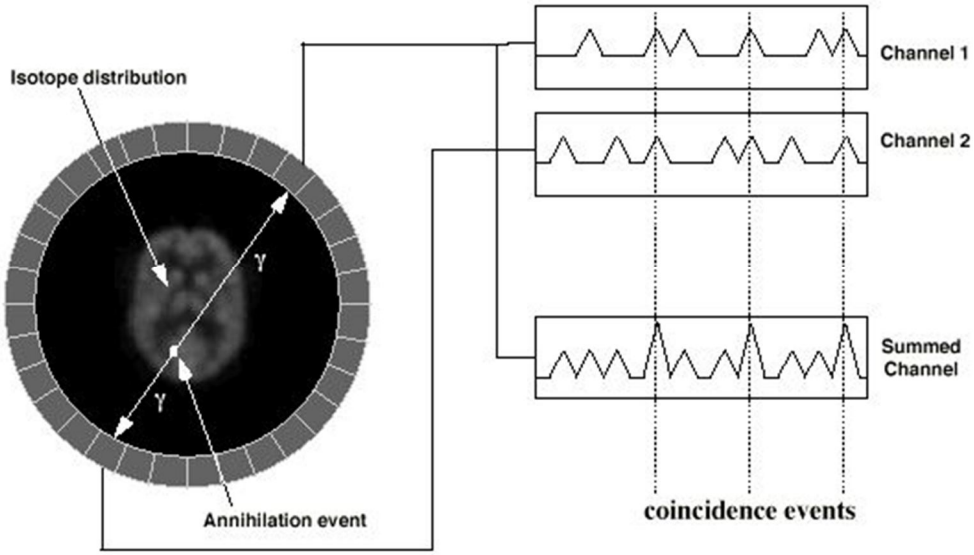

Figure 1.5 Coincidence detection in a PET camera

A coincidence event is assigned to a line of response (LOR) joining the two relevant detectors. In this way, positional information is gained from the detected radiation without the need for a physical collimator. This is known as electronic collimation. Electronic collimation has two major advantages over physical collimation. These are improved sensitivity and improved uniformity of the point source response function (psrf).

When a physical collimator is used, directional information is gained by preventing photons which are not normal or nearly normal to the collimator face from falling on the detector. In electronic collimation, these photons may be detected and used as signal. This results in a significant gain in sensitivity (typically a factor of 10 for 2D mode PET compared with SPECT). This increase in sensitivity means that typical realizable image resolution in PET is around 5-10 mm, whereas in SPECT it is around 15-20 mm.

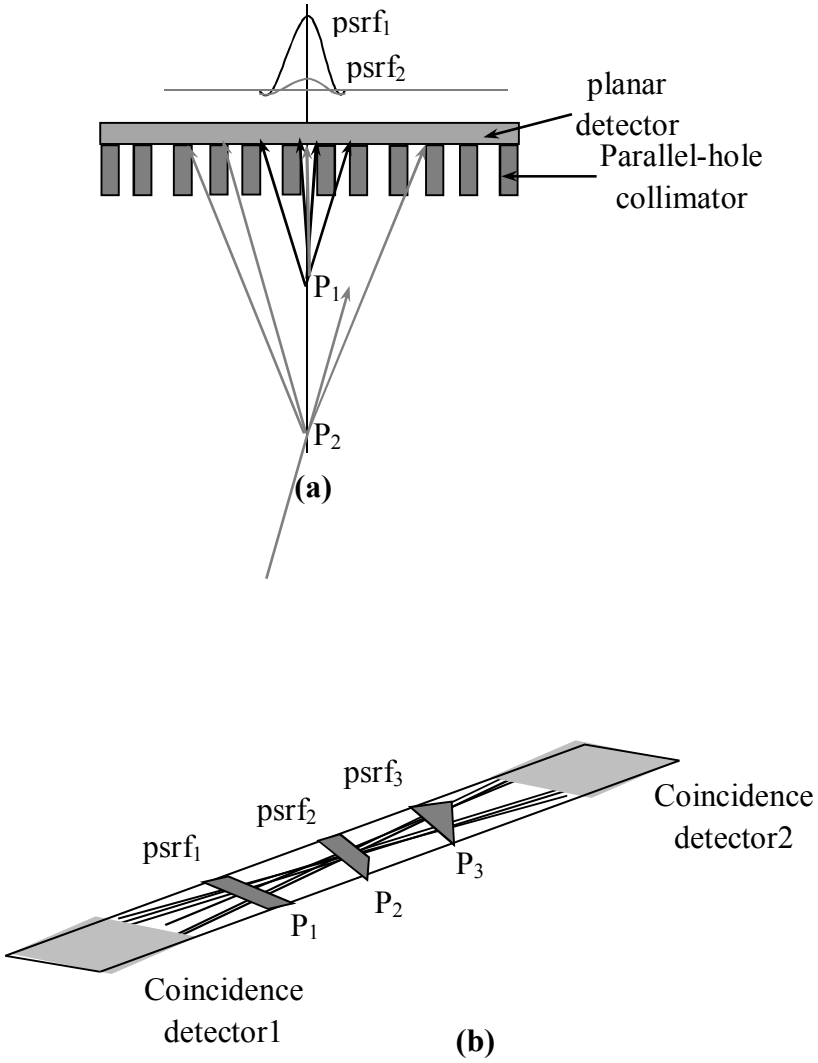

Figure 1.6 Variation of point source response function (psrf) with position P in SPECT and in PET.

In SPECT (a) the FWHM of the psrf increases with increasing distance from the collimator. In PET (b), the FWHM of the psrf varies from one detector width at the edge of the FOV to approximately 1/2 detector width at the center of the FOV

In SPECT, the full-width at half-maximum (FWHM) of the psrf increases with increasing distance of the source from the collimator in figure 1.6 (a) It results in variable resolution in the reconstructed images. In PET, a coincidence event may be detected if the direction of the annihilation photons is constrained to lie along a line-of-sight joining both detector faces. If the annihilation photons are strictly anti-parallel, this results in a psrf which varies in a similar way to that shown in figure 1.6 (b). This constraint is relaxed somewhat because of the small uncertainty in the

direction of the annihilation photons, and in practice the psrf changes only very slightly in the central third of the FOV (Phelps et al 1986) [10]. As a result, the resolution of reconstructed PET images is more uniform than is the case for SPECT images.

1.14 Photon interactions in human tissue and correction for gamma-ray attenuation.

The most important interactions which photons resulting from the positron annihilation undergo in human tissue are Compton scattering and photoelectric absorption.

In Compton scattering a photon interacts with an electron in the absorber material. In the process the kinetic energy of the electron is increased, and the direction of the photon is changed. The energy of the photon after interaction is given by (Evans, 1955) [8].

$$E' = \frac{E}{1 + (E / m_0 c^2)(1 - \cos\theta)} \tag{1.5}$$

Where E is the energy of the incident photon, E' is the energy of the scattered photon, $m_0 c^2$is the rest mass of the electron and θ is the scattering angle. Equation (1.5) implies that quite large deflections can occur with quite small energy loss - for example, for 511 keV photons, a Compton scattering event in which 10% of the photon energy is lost will result in a deflection of just over 25 degrees.

In photoelectric absorption a photon is absorbed by an atom and in the process an electron is ejected from one of its bound shells. The probability of photoelectric absorption increases rapidly with increasing atomic number of the absorber atom, and decreases rapidly with increasing photon energy (Evans, 1955) [8]. In water, the probability of photoelectric absorption decreases with roughly the 3rd power of the photon energy and is negligible at 511 keV (Johns and Cunningham 1983) [11].

The total probability that a photon of a particular energy will undergo some kind of interaction with matter when travelling unit distance through a particular substance is called the linear attenuation coefficient μ of that substance. If I_0 is the

initial intensity of *a* parallel beam of monoenergetic photons, then the intensity $I(x)$ at *a* distance *x* through some attenuating object will be given by (Evans 1955) [8]:

$$I(x) = I_0 e^{-\int_0^x \mu(x)dx} \tag{1.6}$$

Provided scattered photons are removed from the beam. This relation has important consequences for PET. Consider a small volume v in an attenuating object, located at a distance x' along an LOR joining two detectors in the FOV of a PET camera (Figure1.7). Let the volume *v* contain some positron emitting substance, so that there is a flux of 511 keV photons along the line of response joining detector 1 and detector 2. If the linear attenuation coefficient at a point *x* along the LOR is $\mu(x)$, and a is the distance between detectors 1 and 2, it can be explained as;

Probability of a photon reaching detector 1 from P_1 is:

$$P_1 = e^{-\int_0^x \mu(x)dx} \tag{1.7}$$

Probability of a photon reaching detector 2 from P_2 is:

$$P_2 = e^{-\int_x^a \mu(x)dx} \tag{1.8}$$

The probabilities are independent of each other, and both photons must reach the detectors for a coincidence to be recorded. The probability of *a* coincidence *Pc*, is the product of P_1 and P_2

$$P_c = P_1 P_2 = e^{-\int_0^a \mu(x)dx} \tag{1.9}$$

So the quantity (1- P_c) which is the attenuation factor of the photons travelling along the LOR from v is the same for any position along the line of response. By measuring the coincidence signal as a positron-emitting source is moved around the object within the FOV, it is possible to obtain attenuation factors for each LOR. In principle, this enables quantitative measurements of isotope distribution to be made. In SPECT techniques, where the attenuation factors increase with increasing distance from the detectors, there is no simple way to correct for photon attenuation.

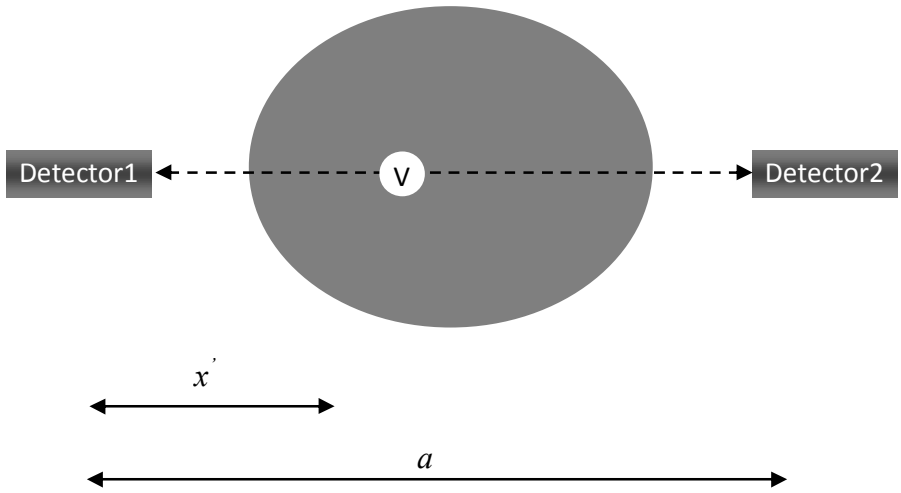

Figure 1.7 Coincidence detection in an attenuating object

For 511 keV photons in human tissue the half-value layer (the distance a beam of photons must travel before 50% have interacted) is around 7 cm. Attenuation factors in human studies can rise to around 50 for LORs crossing large dense areas, for example those crossing the shoulders perpendicularly to the sagittal plane.

1.15 Types of coincidence events.

Coincidence events in PET fall into 4 categories: true, scattered, random and multiple. The first three of these are illustrated in Figure 1.8.

True coincidences occur when both photons from an annihilation event are detected by detectors in coincidence, neither photon undergoes any form of interaction prior to detection, and no other event is detected within the coincidence time-window.

A scattered coincidence is one in which at least one of the detected photons has undergone at least one Compton scattering event prior to detection. Since the direction of the photon is changed during the Compton scattering process, it is highly likely that the resulting coincidence event will be assigned to the wrong LOR. Scattered coincidences add a background to the true coincidence distribution which changes slowly with position, decreasing contrast and causing the isotope concentrations to be overestimated. They also add statistical noise to the signal. The

number of scattered events detected depends on the volume and attenuation characteristics of the object being imaged, and on the geometry of the camera.

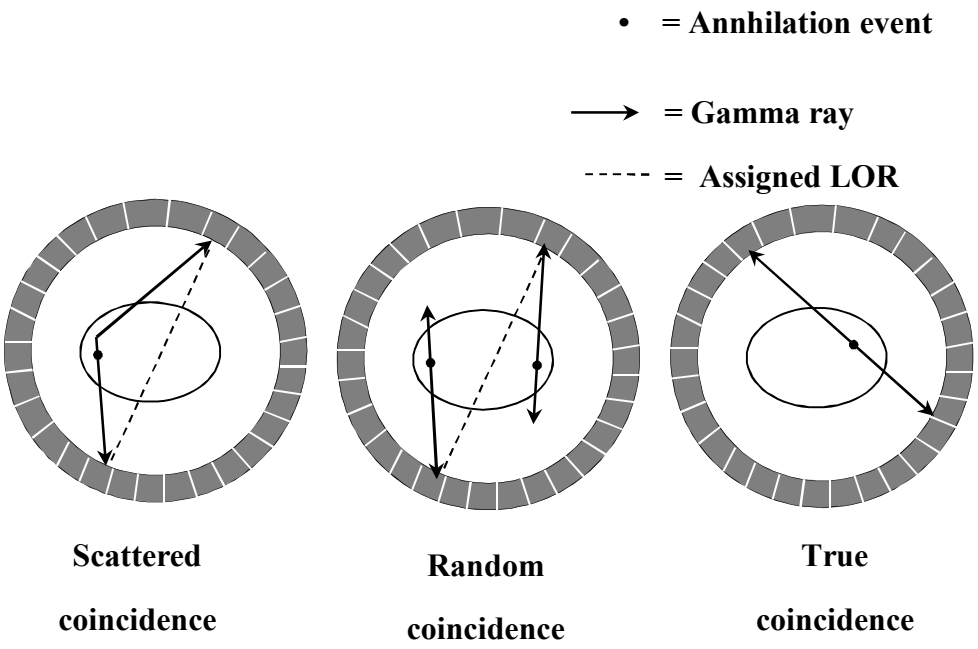

Figure 1.8 Types of coincidences in PET

Random coincidences occur when two photons not arising from the same annihilation event are incident on the detectors within the coincidence time window of the system. The number of random coincidences in a given LOR is closely linked to the rate of single events measured by the detectors joined by that LOR and the rate of random coincidences increase roughly with the square of the activity in the FOV. As with scattered events, the number of random coincidences detected also depends on the volume and attenuation characteristics of the object being imaged, and on the geometry of the camera. The distribution of random coincidences is fairly uniform across the FOV, and will cause isotope concentrations to be overestimated if not corrected for. Random coincidences also add statistical noise to the data.

A simple expression relating the number of random coincidences assigned to an LOR to the number of single events incident upon the relevant detectors can be derived as follows:

Define *t*, the coincidence resolving time of the system, such that any events detected with a time difference of less than t are considered to be coincident. Let r_1

be the single event rate (singles rate) on detector channel 1. Then in one second, the total time-window during which coincidences will be recorded is *2t* r_1 if the singles rate on detector channel 2 isr_2, it can be said that the number of random coincidences R_{12} assigned to the LOR joining detectors *1* and *2* is given by

$$R_{12} = 2tr_1r_2 \tag{1.10}$$

This relation is true provided that the singles rate is much larger than the rate of coincidence events, and that the singles rates are small compared to the reciprocal of the coincidence resolving time *t*, so that dead-time effects can be ignored.

Multiple coincidences occur when more than two photons are detected in different detectors within the coincidence resolving time. In this situation, it is not possible to determine the LOR to which the event should be assigned, and the event is rejected. Multiple coincidences can also cause event miss-positioning.

1.16 Brain Disorders (Alzheimer's)

PET scans show a very consistent diagnostic pattern for Alzheimer's disease, where certain regions of the brain have decreased metabolism early in the disease. In fact, this pattern often can be recognized several years before a physician is able to confirm the diagnosis and is also used to differentiate Alzheimer's from other confounding types of dementia or depression.

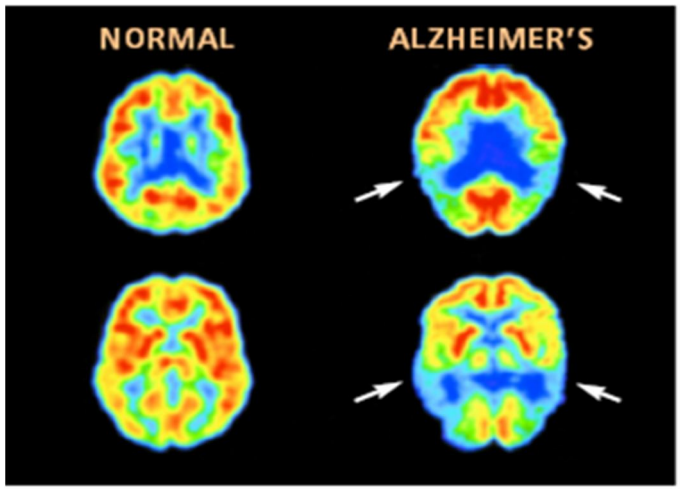

Figure 1.9 Difference of normal brain and Alzheimer's brain

1.17 Brain Disorders (Parkinson's)

PET scans can tell if a patient has Parkinson's disease. F-DOPA a labeled amino acid is used with PET to see if the brain has a deficiency in dopamine production. If it doesn't, then the patient doesn't have Parkinson's disease.

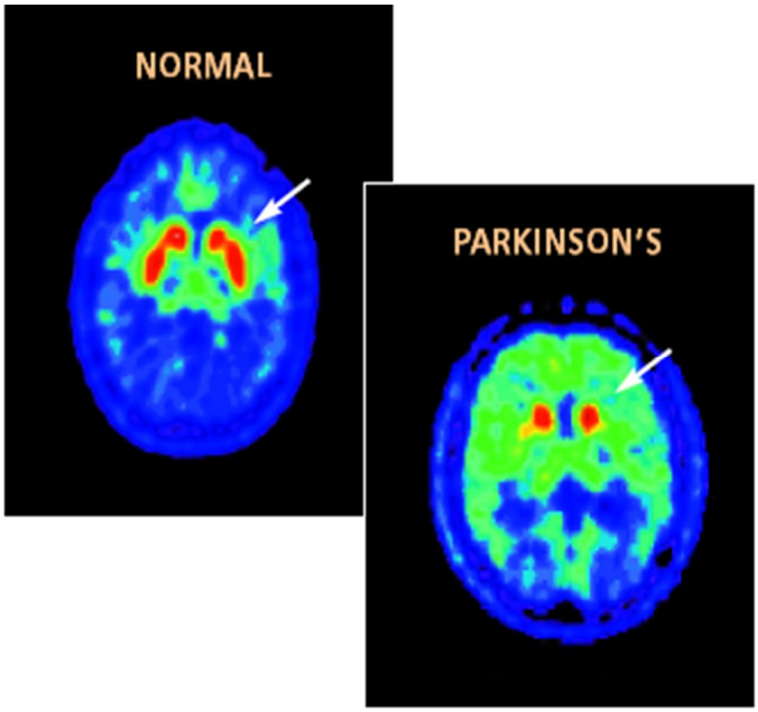

Figure 1.10 Difference of normal brain and Parkinson's brain

1.18 Clinical Applications of PET

Some applications of PET are as follows:

- Cancer:
  - Lung Cancer
  - Colorectal Cancer
  - Breast Cancer
  - Prostate Cancer
- Heart Disease:
  - Coronary Artery Disease
- Brain Disorders:
  - Alzheimer's

    Parkinson's

CHAPTER 2

THEORY

Physics is an experimental science. Experiments provide a substructure to discover physics laws and nature. To develop nuclear and particle physics, experiments are needed. In this world, scattering of the particles gives the main source of information. Several stopping power formulas derived by different researchers are provided in this section.

2.1 Bethe Formula

In theoretical physics and nuclear physics, charged particles passing through nucleus interact with the electrons of atoms in the matter. The interaction results with excitation or ionization of the atom. This results to an energy loss of the charged particle particle. The Bethe formula [12] gives the energy loss per distance travelled of charged particles (alpha particles, protons, atomic ions, not electron) circling atom (or, directly, the stopping power of the matter). Hans Bethe found the relativistic version in 1930, and then, in 1932 the relativistic formula was developed by him [13].

2.1.1 The formulation

The relativistic version of the formula is that:

$$-\frac{dE}{dx} = \frac{4\pi}{m_e c^2} \cdot \frac{nz^2}{\beta^2} \cdot \left(\frac{e^2}{4\pi\varepsilon_0}\right)^2 \cdot \left[ln\left(\frac{2m_e c^2 \beta^2}{I.(1-\beta^2)}\right) - \beta^2\right] \qquad (2.1)$$

Where

$$\beta = {}^{\upsilon}/_{c} \qquad (2.2)$$

υ : particle velocity

e : particle energy

x : distance moved by the charge particle

c : speed light

z : particle charge

e : electron charge

m_e: electron rest mass

n : electron density of the target materia

I : mean excitation potential

ε_0: vacuum permittivity

The electron density of the matter can be calculated as;

$$n = \frac{N_A.Z.\rho}{A.M_A} \tag{2.3}$$

Where

ρ : the material density,

Z : the atomic number and A is the mass number,

N_A : the Avogadro's number and M_A is the molar mass constant.

At low energies, in other words, for little velocities of the particle ($\beta<<1$), Bethe formula [12] is converted to

$$-\frac{dE}{dx} = \frac{4\pi nz^2}{m_e v^2} \cdot \left(\frac{e^2}{4\pi\varepsilon_0}\right)^2 \cdot \left[ln\left(\frac{2m_e v^2}{I}\right)\right] \tag{2.4}$$

At low energies, according to the Bethe formula, stopping power shows a graph downward with increasing energy approximately as $1/v^2$. It decreases a minimum for approximately. $E=3mc^2$, where m is the particle mass (for protons, it is approximately 3000 MeV). At high energies (relativistic cases , $\beta \approx 1$), due to the transversal component of the electric field, stopping power increases again, logarithmically.

2.1.2 The mean excitation potential

According to the Bethe formula [12], the matter is clearly defined by a single number, that is the mean excitation potential I. It is shown that the mean ionization potential of atoms is nearly obtained by [14].

$$I=(10eV).Z \tag{2.5}$$

Where Z is the atomic number of the atoms of the matter. If this approximation is used in the equation (2.1), Bethe-Bloch formula can be obtained.

2.1.3 Corrections to the Bethe formula

The Bethe formula [12] is used only high energies so that the charged atomic particle (the ion) does not carry any atomic electrons with it. For smaller energies, when the ion carries electrons, this reduces its charge effectively, and the stopping power is therefore decreased. However, if the atom is fully ionized, again corrections must be done.

With supporting of the quantum mechanical perturbation theory, Bethe found the formula [12]. Thus, his outcomes is directly proportional to the square of the charge of the particle. The definition can be developed by calculating corrections which uses the higher powers of z. These corrections are: the Barkas-Andersen-effect (proportional to z^3, after Hans Henrik Andersen and Walter H. Barkass), and the Bloch-correction (proportional to z^4), and also, it must be known that the atomic electrons are not stable ("shell correction").

2.2 R. K. BATRA and M. L. SEHGAL Formula

2.2.1 The procedure

The calculation of the positron-electron ratio of the penetration range is based on the idea that both the inelastic and elastic interactions of these particles with matter should be properly taken into account. Firstly the multiple scattering effects are ignored. Then, following the usual definition of the average range of a charged particle of initial energy *E,* the ratio of the positron range $R^+$to the electron range$R^-$is written as

$$\frac{R^{+}(E)}{R^{-}(E)} = \frac{\int_0^E \left[-\frac{1}{\rho}\left(\frac{dE}{dx}\right)_{tot}^{+}\right]^{-1} dE}{\int_0^E \left[-\frac{1}{\rho}\left(\frac{dE}{dx}\right)_{tot}^{-}\right]^{-1} dE} \tag{2.6}$$

$$-\frac{1}{\rho}\left(\frac{dE}{dx}\right)_{tot}^{\pm} = -\frac{1}{\rho}\left(\frac{dE}{dx}\right)_{col}^{\pm} - \frac{1}{\rho}\left(\frac{dE}{dx}\right)_{rad}^{\pm} \tag{2.7}$$

Where the upper superscript stands for positrons and the lower for electrons.

2.2.2 Total Energy Loss

Electrons and positrons, in passing through matter, lose their energy by two processes; (i) collision and excitation loss and (ii) bremsstrahlung loss.

2.2.3 Collision and Excitation Loss

The average coIlision loss per unit path length is given as:

$$\left(-\frac{1}{\rho}\cdot\frac{dE}{dx}\right)_{coll}^{\pm} = \frac{2\pi e^4 N_0 Z}{A m_e c^2 \beta^2}\cdot\left[ln\left(\frac{T^2}{I^2}\frac{\gamma+1}{2}\right) + f^{\pm}(\gamma) - \delta\right] \tag{2.8}$$

Where e is the charge of electron or positon; m, the electron mass; A the atomic weight of the scatterer; N, is Avogadro's number; the ratio of the particle velocity to the velocity of light in vacuum; I the average ionization potential energy; $E = \gamma mc^2$ is the total incident energy; $T = (\gamma - 1)mc^2$ is the kinetic energy of the moving electron and δ is the density effect correction.

2.2.4 Bremsstrahlung Loss

When an electron traverses a foil of thickness dx, the average energy lost due to radiation is given by

$$\left(-\frac{dE}{dx}\right)_{rad} = NE\Phi_{rad}, \tag{2.9}$$

$$\emptyset_{rad} = \frac{1}{E}\int_0^T k d\sigma_K \tag{2.10}$$

Where k is the energy of the emitted photon in units of $m_e c^2$; N the number of atoms per cm^3 and do, the corrected differential form of the bremsstrahlung crosssection.

2.2.5 Empirical relation.

It is easy to see that the reciprocal of the total stopping power given by the sum of equations. (2.9) and (2.10) does not allow an explicit evaluation of $R^{\pm}$. To overcome this difficulty, R.K.BATRA and M.L.SEHGAL found a convenient empirical relation for the total stopping power of electrons and positrons.[14] It is written as

$$-\frac{1}{\rho}\left(\frac{\mathrm{dE}}{\mathrm{dx}}\right)_{\mathrm{tot}}^{\pm} = (\mathrm{mZ} + \mathrm{c})\mathrm{F}^{\pm}(\gamma) \qquad (2.11)$$

$$\mathrm{F}^{+}(\gamma)=\frac{\gamma^{2.4}}{\gamma^{1.9}-1} \qquad (2.12)$$

$$\mathrm{F}^{-}(\gamma)=\frac{\gamma^{2.56}}{\gamma^{2}-1} \qquad \text{for } \mathrm{T}\leq 500\mathrm{keV} \qquad (2.13)$$

Where A and ρ denote the atomic number and density of the stopping material respectively. The appropriate values of the constants m and c are given in Table 2.1

Table 2.1 Numerical values of m and c

Z-values	***m***	***c***
	$(\mathbf{g.cm^{-2}.MeV^{-1}})$	$(\mathbf{g.cm^{-2}.MeV^{-1}})$
Z≤38	-0.00595	0.9280
Z≥38	-0.00285	0.8100

2.3 S.K. GUPTA et al. Formula

Recently S. K. GUPTA, J. C. GOVIL, R. K. TYAGI and O. P. VARMA reported modified emprical equations for the stopping power [15].

For stopping power of positron and c.s.d.a. range difference of positrons , emprical relations have been derived in the energy region 0.2 to 10 Mev.These formulas are used for elements of atomic numbers between 1 to 92.

The formula is that:

$$\left(-\frac{1}{\rho}\cdot\frac{dE}{dx}\right)_{Total} = (SZ + 1.3230)\left[\frac{\gamma^{2}}{\gamma^{az+b}} - 1\right] \qquad (2.14)$$

Where S, a and b are the parameters and

$$\gamma = \left(\frac{\tau}{mc^2}\right) + 1 \qquad (2.15)$$

τ is the incident kinetic energy and mc^2 is the rest mass energy of the positron. ρ is the density of the medium.

Table 2.2 Numerical values of parameters appeared in the equation (2.14) for positron.

Z-values	**(-S) (MeV cm^2/g^*)**	**a**	**b**
$2 \leq Z \leq 10$	0.05458 ± 0.033069		
$10 \leq Z \leq 30$	0.02420 ± 0.0074595	-0.0040	1.8496
$30 \leq Z \leq 92$	0.012924 ± 0.0038202		

g^* is the unit of the mass.

2.4 Nicholas TSOULFANIDIS Formula

Stopping power is expressed by The International Commision on Radiation Units and Measurements or ICRU as the average energy dissipated by ionizing radiation in a medium per unit path length of travel of the radiation in the medium. It is, of course, impossible to predict how a given charged particle will interact with any given atom of the absorber medium. Also, when the coulombic forces of charged particles interact simultaneously with many atoms as it travels through the absorbed medium, it can be predicted as an average effect of energy loss per particle distance of travel. The formulas for the stopping power of charged particles due to coulombic interactions are most clearly defined by Tsoulfanidis (1995) [16] as the following

$$\frac{dE}{dx} = 4\pi r_0^2 \frac{mc^2}{\beta^2} NZ \left[ln\left(\frac{\beta\gamma\sqrt{\gamma-1}mc^2}{I}\right) - \frac{\beta^2}{24}\left(23 + \frac{14}{\gamma+1} + \frac{10}{(\gamma+1)^2} + \frac{4}{(\gamma+1)^3}\right) + \frac{\ln 2}{2}\right] \qquad (2.16)$$

N is the number of atoms per m^3 in the absorber material through which the charged particle travels $(N=\rho(Na/A))$ where ρ is the absorber density in units of g/cm^3. Na is the Avogadro's number A and Z are the atomic weight and atomic number. $\gamma = \frac{(T+mc^2)}{mc^2}$ where T is the particle kinetic energy in Mev and M is the particle rest mass β is the relative phase velocity of the particle.

$$\beta=\gamma/c=\sqrt{1-(\frac{1}{\gamma^2})} \quad (2.17)$$

I is the mean excitation potential of the absorber in units of eV approximated by the equation

$$I=(9.76+58.8Z^{-1.19})Z, \text{ when } Z>12 \quad (2.18)$$

The total stopping power for light charged particles is equal to the sum of both collisional and bremsstrahlung stopping powers.

$$\left(-\frac{dE}{dx}\right)^{\pm}_{tot}=\left(-\frac{dE}{dx}\right)^{\pm}_{coll}+\left(-\frac{dE}{dx}\right)^{\pm}_{rad} \quad (2.19)$$

It can be calculated as the radiative stopping power with above formula;

$$\frac{\left(-\frac{dE}{dx}\right)_{rad}}{\left(-\frac{dE}{dx}\right)_{coll}}\approx\frac{ZE}{800} \quad (2.20)$$

2.5 ROHRLICH and CARLSON Formula

The theory of the mass collision stopping power for heavy charged particles, electrons and positrons as a result of soft and hard collisions combines the Bethe theory [12] for soft collisions with the stopping power as a result of energy transfers due to hard collisions. The result of this, for a heavy charged particle with mass M and velocity γ, where the energy transfer due to hard collisions is limited to $2mc^2\beta^2/(1-\beta^2)$, where $\beta=\gamma/c$, is:

$$\frac{S_{coll}}{\rho}=\frac{4\pi N_A Z}{A}\cdot\frac{r_e^2 m_e c^2}{\beta^2}z^2\left[\ln\left(\frac{2m_e v^2}{I}\right)-\ln(1-\beta^2)-\beta^2-\frac{C}{Z}\right] \quad (2.21)$$

Where

r_e is the classical electron radius (2.82 fm);

Z is the projectile charge in units of electron charge;

I is the mean excitation potential of the medium;

C/Z is the shell correction.

The mean excitation potential I is a geometric mean value of all ionization and excitation potentials of an atom of the absorbing material. Since binding effects influence the exact value of I, calculation models are often in adequate to estimate its

value accurately. Hence, *I* values are usually derived from measurements of stopping powers in heavy charged particle beams, for which the effects of scattering in these measurements is minimal.

For elemental materials *I* varies approximately linearly with *Z*, on average, $I = 11.5\,Z$ for compounds. *I* is calculated assuming additivity of the collision stopping power, taking into account the fraction by weight of each atom constituent in the compound.

The mass stopping power does not depend on the projectile mass and is proportional to the inverse square of the projectile velocity. Note that the term $2m_e c^2$under the logarithm has no relation to the kinetic energy of any of the particles involved in the collision process.

The mass stopping power gradually flat tens to a broad minimum for kinetic energies $E_k = 3mec^2$.

The leading factor *Z*/*A* is responsible for a decrease of about 20% in stopping power from carbon to lead. The term *lnI* causes a further decrease in stopping power with *Z*.

In a given medium, the square dependence on the projectile charge (z^2) causes heavy charged particles with double the charge to experience four times the stopping power.

For electrons and positrons, energy transfers due to soft collisions are combined with those due to hard collisions using the Møller (for electrons) and Bhabba (for positrons) cross-sections for free electrons. ROHRLICH and CARLSON found a formula [17] with the complete mass collisional stopping power for electrons and positrons.

$$\frac{S_{coll}}{\rho} = \frac{N_A Z}{A} \cdot \frac{\pi r_0^2 2m_e c^2}{\beta^2}\left[\ln\left(\frac{E_K}{I}\right)^2 + \ln\left(1+\frac{\tau}{2}\right) + F^{\pm}(\tau) - \delta\right] \tag{2.22}$$

With F^-given for electrons as:

$$F^-(\tau) = (1-\beta^2)\left[1 + \frac{\tau^2}{8} - (2\tau+1)\ln 2\right] \tag{2.23}$$

and F^+given for positrons as:

$$F^+(\tau) = 2\ln 2 - (\beta^2/12)[23 + 14/\tau + 2 + 10/(\tau+2)^2 + 4/(\tau+2)^3] \tag{2.24}$$

In this equation,

$$\tau = E_K/m_e c^2 \text{ and } \beta = \gamma/c$$

2.6 P.B. PAL et al. Formula

Simple empirical formula for the total stopping power for electrons and positrons in matter have been derived from Wilson's theory by P.B. PAL V.P. VARSHNGEY and D.K. GUPTA [18]. The Formulae are valid for electrons and positrons in the energy region from 5 to 1000 MeV in absorbers of atomic number from Z = 1 to 92. Values of the total stopping power, obtained by the present approach are compared with the theoretical values. The presented formulae yield good approximate values of the total stopping power for electrons and positrons in matter within an accuracy of +10%.

2.6.1 Introduction

The knowledge of the total stopping power for electrons and positrons in matters is an effective tool for understanding their interaction mechanism with matter. Electrons and positrons during transmission through matter lose their energy mainly in two processes of collision with atomic electrons (i) nonradiative collision and (ii) radiative collision.

In this study, the Wilson theory was used to derive simple formulae for the total stopping power for electrons and positrons valid in the energy region from 5 to 1000 MeV in elemental and compound absorbers of atomic number from Z = 1 to 92.

2.6.2 Stopping power formula

In the calculation of cascade showers, using Wilson theory a simple analytical expression has been derived for the mean range of high energy positrons.

$$-\frac{1}{\rho}\left(\frac{d\gamma}{dx}\right)^{\pm} = (MZ+N)(P_0^{\pm} + P_1^{\pm}\gamma) \tag{2.25}$$

Where M and N are the parameters which have the same value as given by Batra and Sehgal to the parameters m and c respectively, P_0,and P_1 are the parameters expressed as

$$P_n^{\pm} = A_n^{\pm} + B_n^{\pm} Z + C_n^{\pm} Z^2 \tag{2.26}$$

Where n = 0 and 1, and A, B,and C are the coefficients . Equation (2.25) is valid for absorbers of atomic number Z >10. The stopping power for electrons and positrons in absorbers of Atomic number Z < 10 is given by

$$-\frac{1}{\rho}\left(\frac{d\gamma}{dx}\right)^{\pm} = \left(\frac{2Z}{a}\right).(MZ+N)(P_0^{\pm} + P_1^{\pm}\gamma) \qquad (2.27)$$

Table 2.3 Numerical values of the coefficients A_n^-,B_n^-,C_n^-

E (MeV)	**Z**	**n**	$\boldsymbol{A_n^-}$ **(x 10^{-5})**	$\boldsymbol{B_n^-}$ **(x 10^{-3})**	$\boldsymbol{C_n^-}$ **(x 10^{-5})**
$5 \le E \le 10^3$	$1 \le Z \le 64$	0	139170	2.7254	-
		1	8.4321	1.7373	-
	$64 \le Z \le 92$	0	158127.37	-6.2779	9.40594
		1	002291.49	+0.720386	1.0329

Table 2.4 Numerical values of the coefficients A_n^+,B_n^+,C_n^+

E (MeV)	**Z**	**n**	$\boldsymbol{A_n^+}$ **(x 10^{-3})**	$\boldsymbol{B_n^+}$ **(x 10^{-3})**	$\boldsymbol{C_n^+}$ **(x 10^{-5})**
$5 \le E \le 10$	$1 \le Z \le 92$	0	1358.0481	3.16801	-
		1	4.55151	1.38636	-
$10 \le E \le 10^3$	$1 \le Z \le 92$	0	1421.4145	1.22493	-8.7690
		1	1.02208	1.52484	+0.381085

Table 2.5 Values of the parameters *M* and *N*

Atomic Number	**M (MeV cm^2/g)**	**N (MeV cm^2/g)**
$1 \le Z \le 10$	-0.0330	1.3230
$10 \le Z \le 36$	-0.0097	1.0911
$36 \le Z \le 92$	-0.0048	0.9156

CHAPTER 3

RESULTS and DISCUSSIONS

Our objective in this work was to determine the stopping powers of positron in different materials using different formulas developed by the researchers and to compare the results with each other. For this purpose we selected five elements in our calculations. These are Al, Si, Cu, Pb and Ag.

The results of stopping power calculations of positron in Al, Si, Cu, Ag, and Pb are provided in this section in Tables 3.1-3.5 and in Figures 3.1 and 3.10. We presented the stopping powers as function of positron energy in two plots for two energy ranges: one is between 0 and 1 MeV and the other is between 1 MeV and 50 MeV for all materials. The reason is that the effect of positron energy on the stopping powers can be more clearly observed. It is clearly seen from the Tables 3.1-3.5 and Figures 3.1-3.10 that the stopping power is very effective at low energy and it decreases as the energy of positron increases. It reaches a minumum value and then starts increasing with the increase in positron energy. This observation is true for all materials used in this work.

The increase in the stopping power after reaching its minimum value as the energy increases is due to the energy loss in terms of Bremsstrahlung radiation of positrons since the energy loss in terms of Bremsstrahlung at high energy is very dominant with respect to the Coulombic energy loss.

We made the stopping power calculations for positrons in five materials using Rohrlich and Carlson and Tsoulfanidis equations for all energy ranges, hovewer using Batra and Sehgal, Gupta et al., and P. B. Pal et.al. for certain energy ranges since they are not valid for all energy ranges. Batra and Sehgal equation is valid from 0.0 to 0.5 MeV, Gupta et al. from 0.2 to 10 MeV, and P. B. Pal et al. from 5 Mev to 50 Mev. It is obvious from the Tables 3.1-3.5 that Rohrlich and Carlson and Tsoulfanidis equations give better results with compared to the theoretical values at

low energies up to 1.0 MeV. It seems that Gupta et al. method provides closer results to the theoretical results between 1.0 MeV to 10 MeV, while P. B. Pal et al. method gives better results from 5 MeV to 50 MeV. These interpretations are true for all investigated materials.

Table 3.1 Stopping powers of positrons in Al obtained by different methods.

Energy	Theoretical value $\left(\frac{MeV.cm^2}{g}\right)$	Rohrlich and Carlson $\left(\frac{MeV.cm^2}{g}\right)$	Tsoulfanidis $\left(\frac{MeV.cm^2}{g}\right)$	Batra and Sehgal $\left(\frac{MeV.cm^2}{g}\right)$	Gupta et al. $\left(\frac{MeV.cm^2}{g}\right)$	P.B.Pal et al. $\left(\frac{MeV.cm^2}{g}\right)$
20 **kev**	10,80	10,88	10,84	12,33	-	-
30	7,90	7,96	7,94	8,52	-	-
40	6,36	6,40	6,38	6,62	-	-
50	5,38	5,42	5,41	5,48	-	-
60	4,72	4,75	4,74	4,73	-	-
70	4,23	4,26	4,25	4,19	-	-
80	3,85	3,88	3,88	3,79	-	-
90	3,56	3,58	3,58	3,48	-	-
100	3,32	3,34	3,34	3,23	-	-
150	2,59	2,61	2,61	2,50	-	-
200	2,22	2,24	2,24	2,15	2,41	-
250	2,00	2,02	2,02	1,96	2,14	-
300	1,85	1,88	1,88	1,83	1,96	-
350	1,75	1,78	1,78	1,76	1,84	-
400	1,68	1,70	1,71	1,70	1,75	-
450	1,63	1,65	1,65	1,67	1,69	-
500	1,59	1,61	1,61	1,65	1,64	-
600	1,53	1,56	1,56	-	1,57	-
700	1,49	1,53	1,53	-	1,52	-
900	1,46	1,50	1,50	-	1,48	-
1 **MeV**	1,45	1,49	1,49	-	1,46	-

Table 3.1 (continued)

1,5	1,45	1,50	1,50	-	1,45	-
2	1,48	1,54	1,54	-	1,48	-
2,5	1,50	1,58	1,58	-	1,51	-
3	1,53	1,62	1,62	-	1,54	-
3,5	1,56	1,66	1,66	-	1,57	-
4	1,59	1,70	1,70	-	1,60	-
4,5	1,62	1,74	1,73	-	1,63	-
5	1,64	1,77	1,77	-	1,65	1,59
10	1,87	2,08	2,07	-	1,87	1,80
15	2,09	2,34	2,34	-	-	2,00
20	2,29	2,59	2,58	-	-	2,21
25	2,50	2,82	2,82	-	-	2,41
30	2,70	3,05	3,05	-	-	2,61
35	2,90	3,28	3,28	-	-	2,81
40	3,10	3,51	3,50	-	-	3,02
45	3,30	3,73	3,73	-	-	3,22
50	3,50	3,96	3,95	-	-	3,42

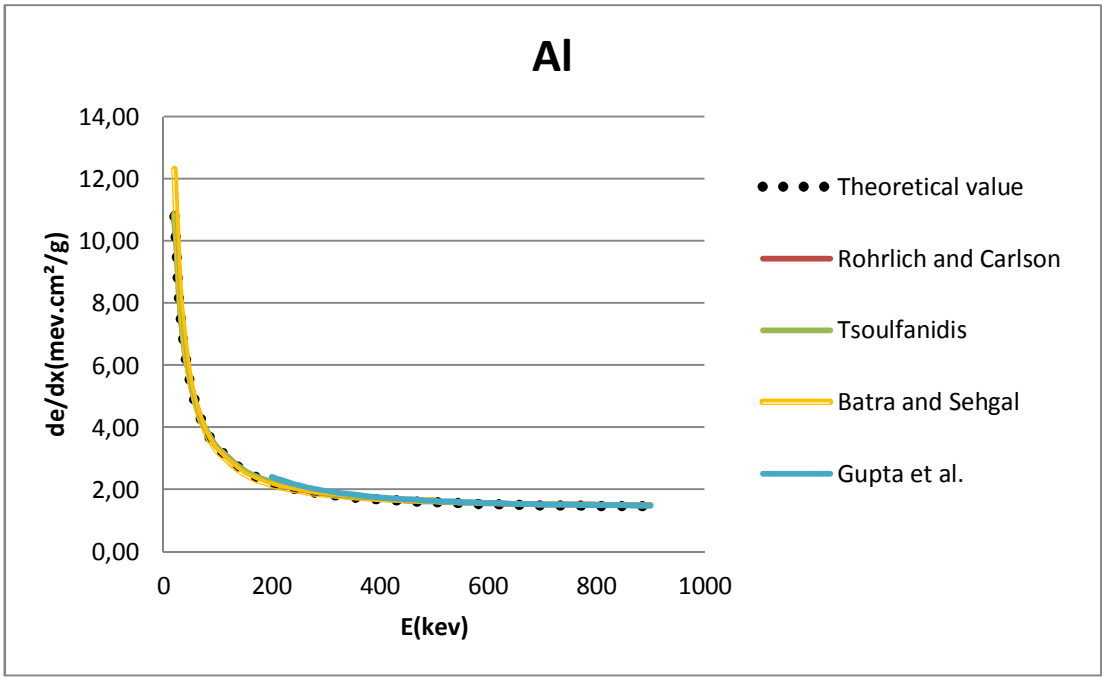

Figures 3.1 Stopping powers of positrons in Al obtained by different methods of as a function of positron energy from 0 to 1 MeV.

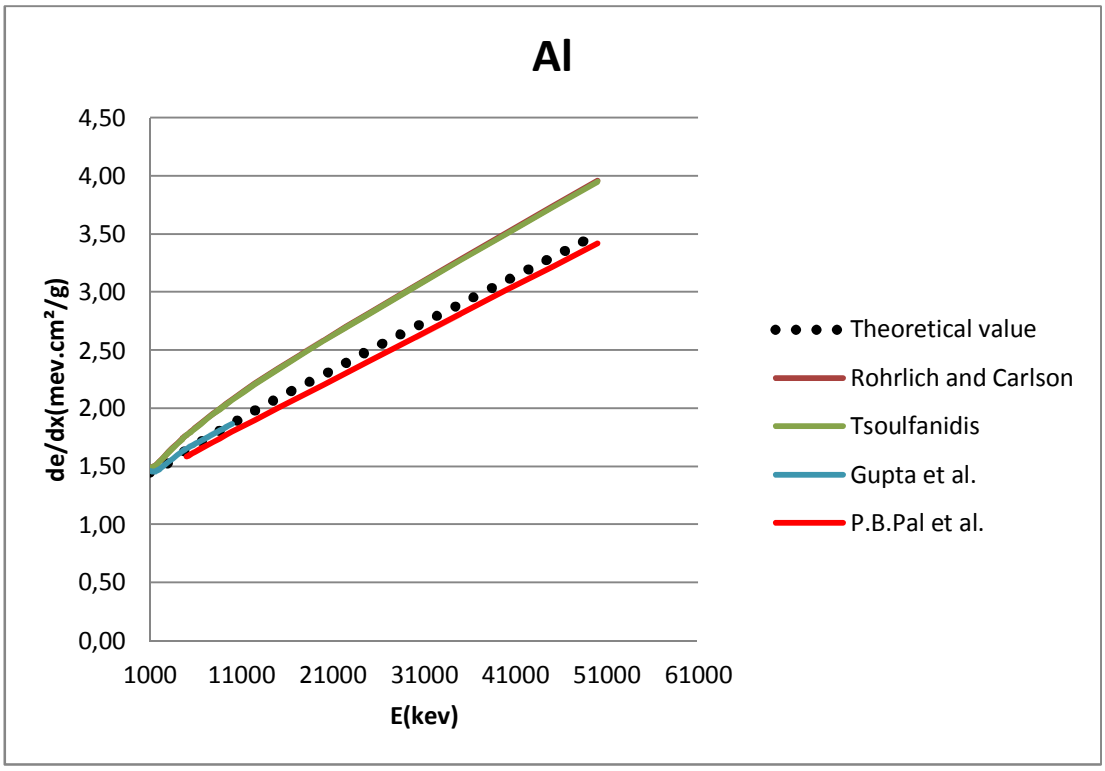

Figures 3.2 Stopping powers of positrons in Al obtained by different methods of as a function of positron energy from 1 to 50 MeV.

Table 3.2 Stopping powers of positrons in Si obtained by different methods.

Energy	Theoretical value $\left(\frac{MeV.cm^2}{g}\right)$	Rohrlich and Carlson $\left(\frac{MeV.cm^2}{g}\right)$	Tsoulfanidis $\left(\frac{MeV.cm^2}{g}\right)$	Batra and Sehgal $\left(\frac{MeV.cm^2}{g}\right)$	Gupta et al. $\left(\frac{MeV.cm^2}{g}\right)$	P.B.Pal et al. $\left(\frac{MeV.cm^2}{g}\right)$
20 **kev**	11,09	11,15	11,15	12,24	-	-
30	8,12	8,16	8,16	8,46	-	-
40	6,53	6,57	6,57	6,57	-	-
50	5,53	5,56	5,57	5,45	-	-
60	4,85	4,88	4,88	4,70	-	-
70	4,35	4,37	4,38	4,16	-	-
80	3,96	3,99	3,99	3,76	-	-
90	3,66	3,68	3,69	3,45	-	-
100	3,41	3,44	3,44	3,21	-	-
150	2,66	2,68	2,69	2,48	-	-
200	2,28	2,30	2,31	2,14	2,36	-
250	2,06	2,08	2,08	1,94	2,09	-
300	1,91	1,93	1,94	1,82	1,92	-
350	1,81	1,83	1,83	1,74	1,80	-
400	1,73	1,75	1,76	1,69	1,72	-
450	1,68	1,70	1,71	1,66	1,65	-
500	1,63	1,66	1,67	1,64	1,61	-
600	1,57	1,61	1,61	-	1,54	-
700	1,54	1,57	1,58	-	1,49	-
900	1,50	1,54	1,55	-	1,45	-
1 **MeV**	1,49	1,54	1,54	-	1,44	-
1,5	1,50	1,55	1,55	-	1,43	-
2	1,52	1,59	1,59	-	1,45	-
2,5	1,55	1,63	1,64	-	1,48	-
3	1,59	1,68	1,68	-	1,51	-

Table 3.2 (continued)

3,5	1,62	1,72	1,72	-	1,54	-
4	1,65	1,76	1,76	-	1,57	-
4,5	1,68	1,80	1,80	-	1,60	-
5	1,71	1,84	1,84	-	1,63	1,59
10	1,96	2,17	2,17	-	1,85	1,81
15	2,20	2,45	2,45	-	-	2,03
20	2,42	2,72	2,72	-	-	2,24
25	2,65	2,98	2,98	-	-	2,46
30	2,87	3,24	3,23	-	-	2,68
35	3,09	3,49	3,49	-	-	2,89
40	3,31	3,74	3,74	-	-	3,11
45	3,53	3,99	3,99	-	-	3,32
50	3,75	4,24	4,23	-	-	3,54

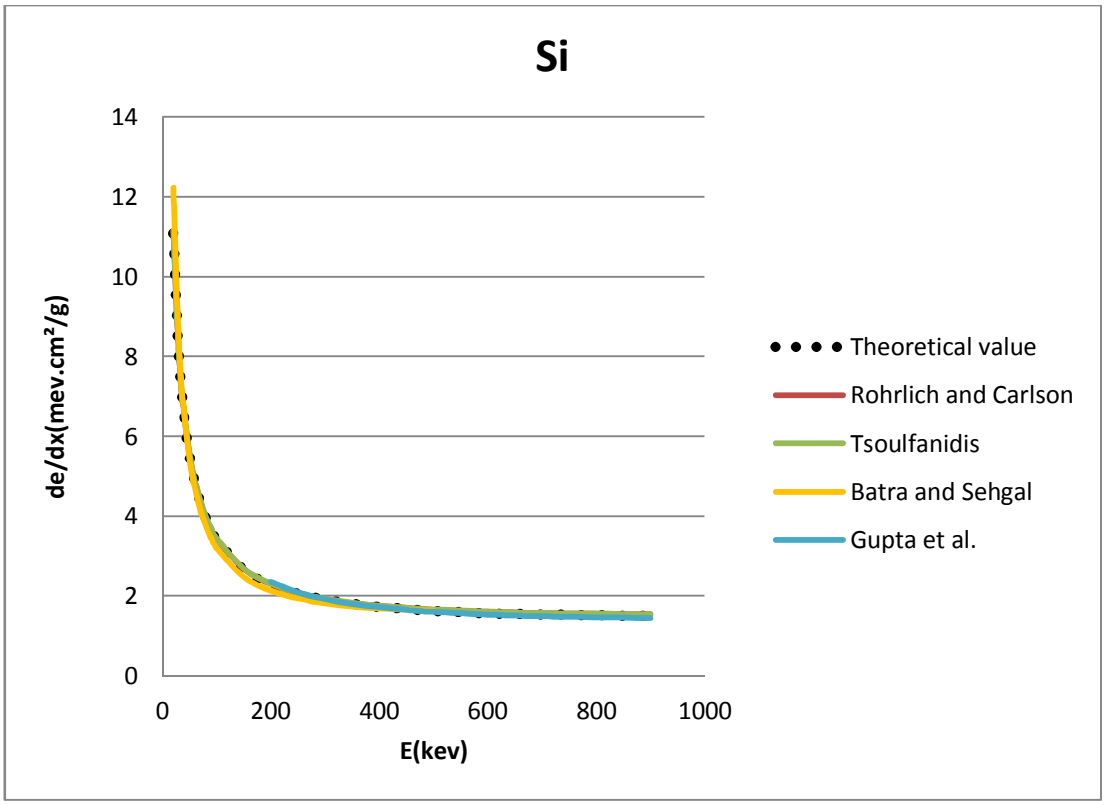

Figures 3.3 Stopping powers of positrons in Si obtained by different methods of as a function of positron energy from 0 to 1 MeV.

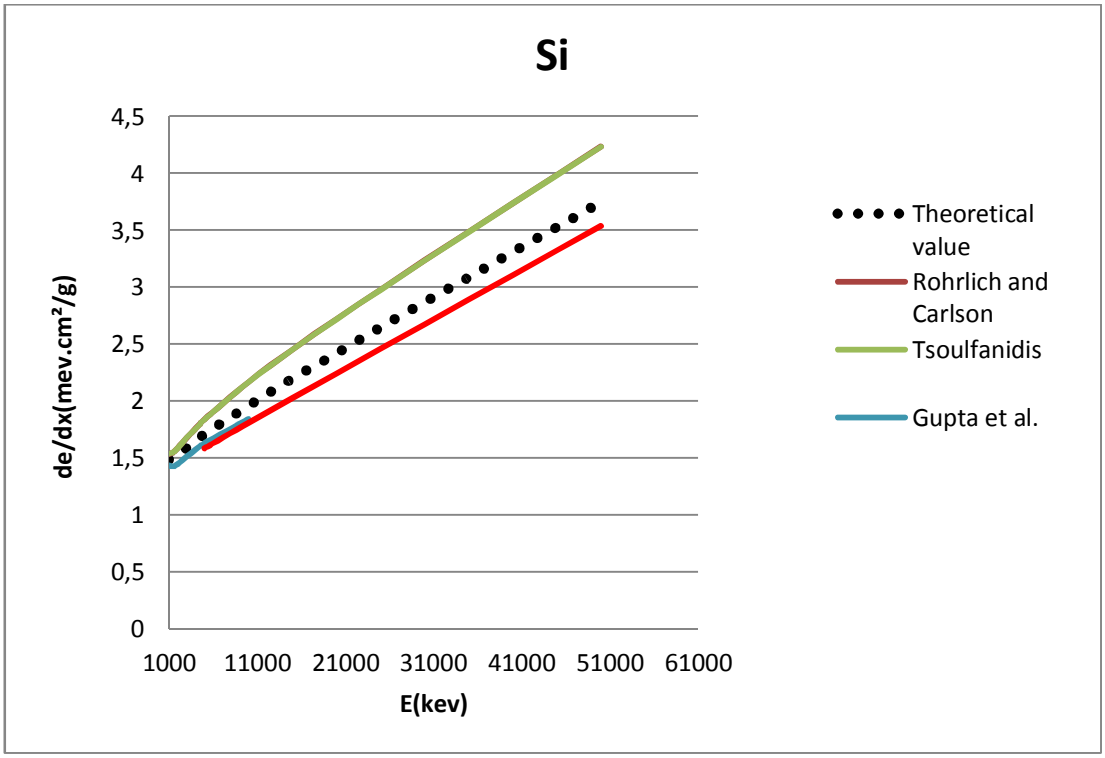

Figures 3.4 Stopping powers of positrons in Si obtained by different methods of as a function of positron energy from 1 to 50 MeV.

Table 3.3 Stopping powers of positrons in Cu obtained by different methods.

Energy	Theoretical value $\left(\frac{MeV.cm^2}{g}\right)$	Rohrlich and Carlson $\left(\frac{MeV.cm^2}{g}\right)$	Tsoulfanidis $\left(\frac{MeV.cm^2}{g}\right)$	Batra and Sehgal $\left(\frac{MeV.cm^2}{g}\right)$	Gupta et al. $\left(\frac{MeV.cm^2}{g}\right)$	P.B.Pal et al. $\left(\frac{MeV.cm^2}{g}\right)$
20 **kev**	8,97	8,87	9,12	10,95	-	-
30	6,62	6,56	6,73	7,57	-	-
40	5,36	5,31	5,45	5,88	-	-
50	4,56	4,52	4,63	4,87	-	-
60	4,00	3,98	4,07	4,20	-	-
70	3,60	3,57	3,66	3,72	-	-
80	3,28	3,27	3,35	3,36	-	-
90	3,04	3,02	3,10	3,09	-	-
100	2,84	2,83	2,89	2,87	-	-
150	2,22	2,22	2,27	2,22	-	-
200	1,91	1,91	1,96	1,91	2,10	-
250	1,72	1,73	1,77	1,74	1,87	-
300	1,60	1,61	1,65	1,63	1,72	-
350	1,51	1,53	1,57	1,56	1,62	-
400	1,45	1,48	1,51	1,51	1,54	-
450	1,41	1,43	1,46	1,48	1,49	-
500	1,37	1,40	1,43	1,46	1,45	-
600	1,33	1,36	1,39	-	1,39	-
700	1,30	1,34	1,37	-	1,36	-
900	1,27	1,32	1,35	-	1,33	-
1 **MeV**	1,27	1,32	1,35	-	1,32	-
1,5	1,28	1,35	1,38	-	1,33	-

Table 3.3 (continued)

2	1,31	1,41	1,43	-	1,37	-
2,5	1,35	1,46	1,48	-	1,41	-
3	1,39	1,52	1,54	-	1,45	-
3,5	1,43	1,57	1,59	-	1,49	-
4	1,47	1,62	1,64	-	1,53	-
4,5	1,51	1,67	1,69	-	1,57	-
5	1,55	1,72	1,74	-	1,60	1,57
10	1,92	2,19	2,21	-	1,88	1,92
15	2,30	2,63	2,65	-	-	2,31
20	2,67	3,05	3,08	-	-	2,69
25	3,04	3,48	3,51	-	-	3,08
30	3,41	3,90	3,94	-	-	3,46
35	3,79	4,33	4,37	-	-	3,85
40	4,16	4,76	4,80	-	-	4,23
45	4,34	5,18	5,23	-	-	4,61
50	4,91	5,62	5,67	-	-	5,00

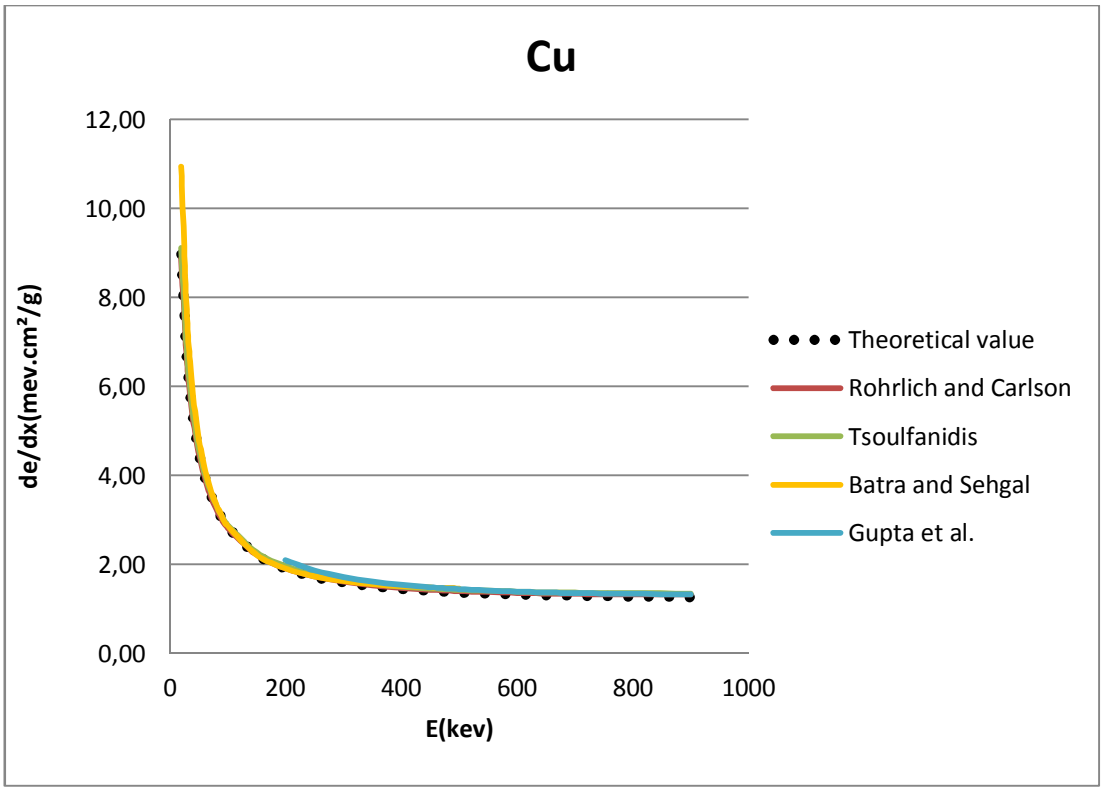

Figures 3.5 Stopping powers of positrons in Cu obtained by different methods of as a function of positron energy from 0 to 1 MeV.

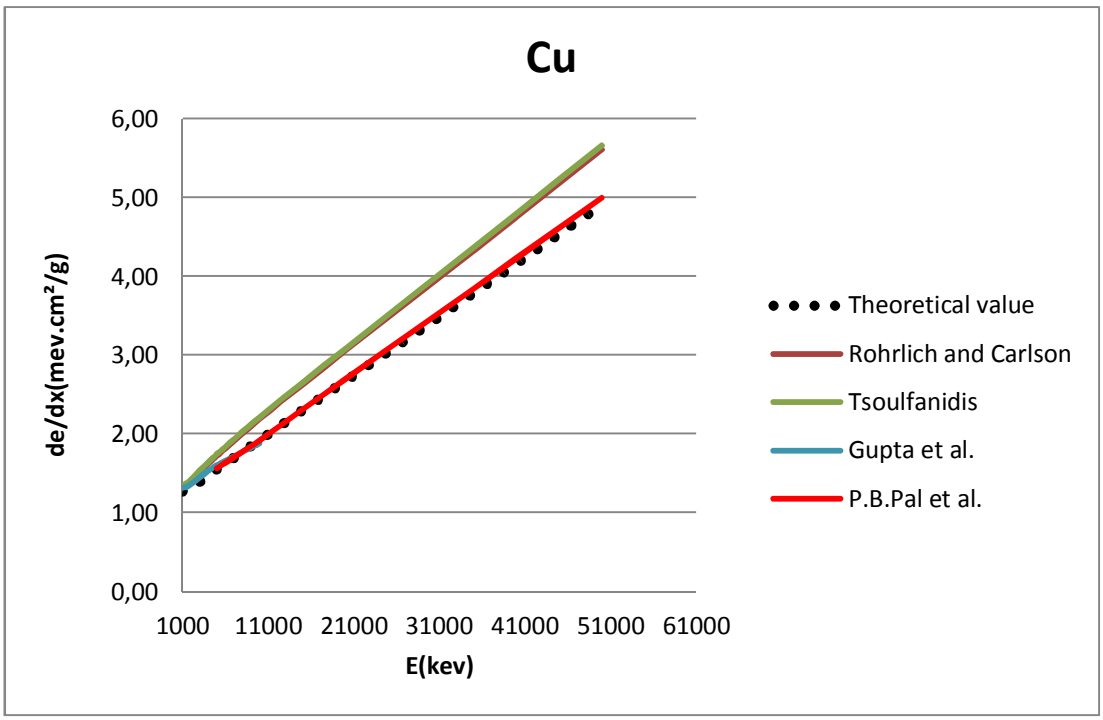

Figures 3.6 Stopping powers of positrons in Cu obtained by different methods of as a function of positron energy from 1 to 50 MeV.

Table 3.4 Stopping powers of positrons in Ag obtained by different methods.

Energy	Theoretical value $\left(\frac{MeV.cm^2}{g}\right)$	Rohrlich and Carlson $\left(\frac{MeV.cm^2}{g}\right)$	Tsoulfanidis $\left(\frac{MeV.cm^2}{g}\right)$	Batra and Sehgal $\left(\frac{MeV.cm^2}{g}\right)$	Gupta et al. $\left(\frac{MeV.cm^2}{g}\right)$	P.B.Pal et al. $\left(\frac{MeV.cm^2}{g}\right)$
20 **kev**	7,88	7,52	7,83	9,80	-	-
30	5,86	5,61	5,82	6,77	-	-
40	4,75	4,56	4,73	5,26	-	-
50	4,05	3,90	4,04	4,36	-	-
60	3,57	3,44	3,56	3,76	-	-
70	3,21	3,10	3,21	3,33	-	-
80	2,94	2,84	2,94	3,01	-	-
90	2,72	2,63	2,72	2,76	-	-
100	2,54	2,46	2,55	2,57	-	-
150	2,00	1,95	2,01	1,99	-	-
200	1,72	1,68	1,74	1,71	1,89	-
250	1,56	1,53	1,58	1,55	1,69	-
300	1,45	1,43	1,47	1,46	1,56	-
350	1,37	1,36	1,40	1,40	1,47	-
400	1,32	1,31	1,35	1,35	1,41	-
450	1,28	1,28	1,32	1,33	1,36	-
500	1,25	1,25	1,29	1,31	1,33	-
600	1,22	1,22	1,26	-	1,28	-
700	1,19	1,20	1,24	-	1,26	-
900	1,18	1,20	1,23	-	1,24	-
1 **MeV**	1,17	1,20	1,23	-	1,24	-
1,5	1,20	1,25	1,28	-	1,27	-
2	1,25	1,31	1,34	-	1,32	-

Table 3.4 (continued)

2,5	1,30	1,38	1,41	-	1,38	-
3	1,35	1,45	1,47	-	1,43	-
3,5	1,40	1,51	1,54	-	1,49	-
4	1,45	1,58	1,61	-	1,54	-
4,5	1,50	1,64	1,67	-	1,59	-
5	1,55	1,71	1,74	-	1,63	1,56
10	2,05	2,32	2,36	-	2,00	2,03
15	2,54	2,92	2,97	-	-	2,59
20	3,05	3,52	3,57	-	-	3,13
25	3,56	4,13	4,18	-	-	3,68
30	4,08	4,73	4,80	-	-	4,23
35	4,60	5,35	5,42	-	-	4,78
40	5,13	5,96	6,04	-	-	5,32
45	5,66	6,59	6,67	-	-	5,87
50	6,19	7,21	7,30	-	-	6,42

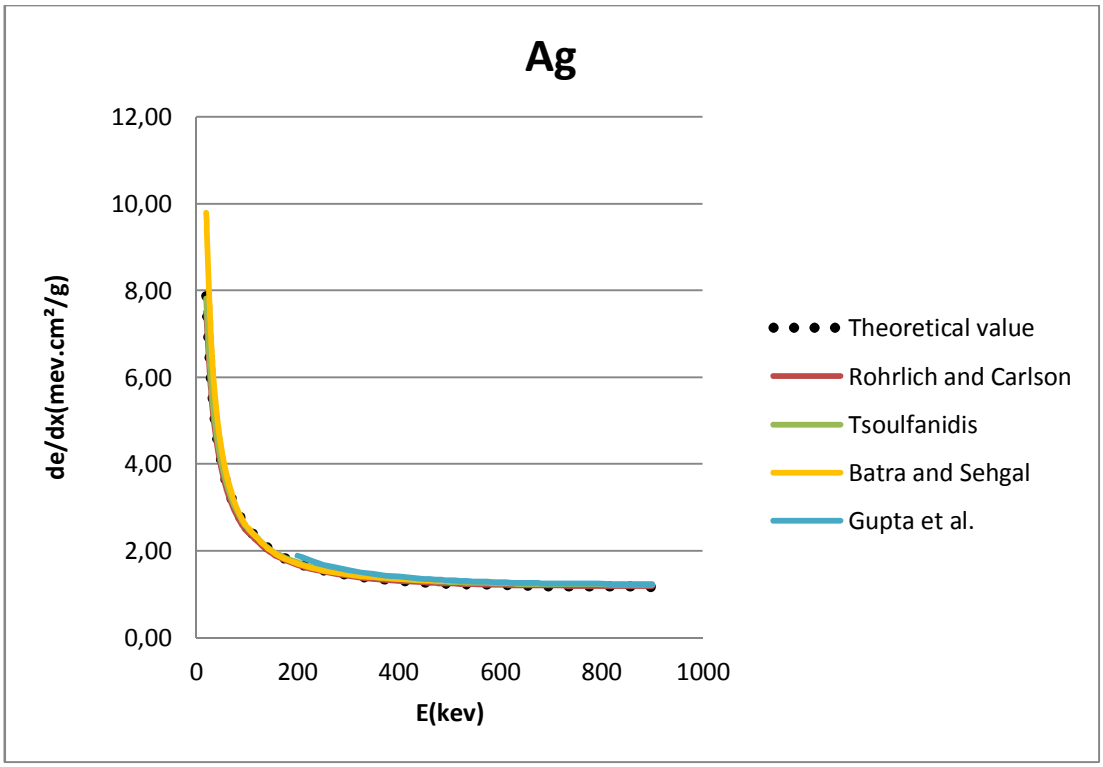

Figures 3.7 Stopping powers of positrons in Ag obtained by different methods of as a function of positron energy from 0 to 1 MeV.

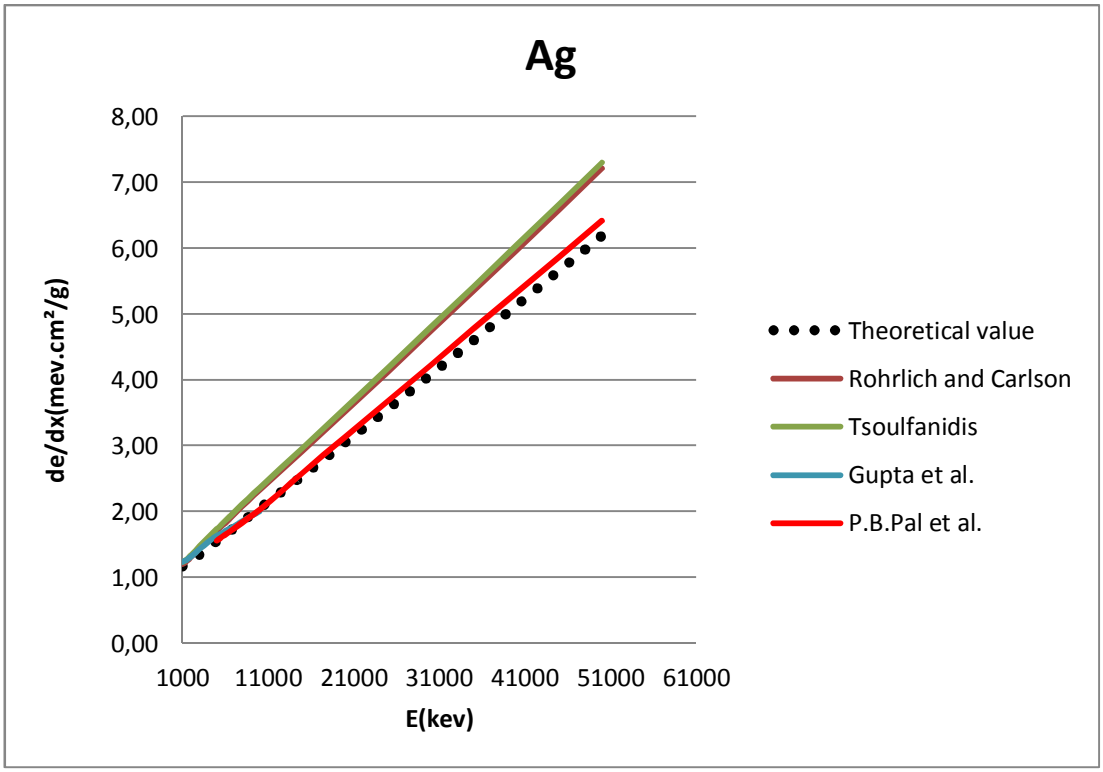

Figures 3.8 Stopping powers of positrons in Ag obtained by different methods of as a function of positron energy from 1 to 50 MeV.

Table 3.5 Stopping powers of positrons in Pb obtained by different methods.

Energy	Theoretical value $\left(\frac{MeV.cm^2}{g}\right)$	Rohrlich and Carlson $\left(\frac{MeV.cm^2}{g}\right)$	Tsoulfanidis $\left(\frac{MeV.cm^2}{g}\right)$	Batra and Sehgal $\left(\frac{MeV.cm^2}{g}\right)$	Gupta et al. $\left(\frac{MeV.cm^2}{g}\right)$	P.B.Pal et al. $\left(\frac{MeV.cm^2}{g}\right)$
20 **kev**	6,24	5,93	6,26	8,35	-	-
30	4,69	4,48	4,71	5,77	-	-
40	3,83	3,68	3,86	4,49	-	-
50	3,28	3,16	3,31	3,72	-	-
60	2,90	2,80	2,93	3,20	-	-
70	2,62	2,53	2,64	2,84	-	-
80	2,40	2,32	2,43	2,57	-	-
90	2,23	2,16	2,25	2,36	-	-
100	2,09	2,02	2,11	2,19	-	-
150	1,66	1,61	1,68	1,69	-	-
200	1,44	1,40	1,46	1,46	1,71	-
250	1,30	1,28	1,33	1,32	1,53	-
300	1,22	1,20	1,25	1,24	1,42	-
350	1,16	1,15	1,19	1,19	1,35	-
400	1,12	1,11	1,16	1,15	1,30	-
450	1,09	1,09	1,13	1,13	1,26	-
500	1,07	1,07	1,11	1,12	1,24	-
600	1,04	1,05	1,09	-	1,21	-
700	1,03	1,04	1,08	-	1,19	-
900	1,02	1,05	1,08	-	1,19	-
1 **MeV**	1,03	1,06	1,09	-	1,20	-
1,5	1,07	1,13	1,16	-	1,27	-
2	1,12	1,21	1,24	-	1,35	-

Table 3.5 (continued)

2,5	1,18	1,29	1,33	-	1,44	-
3	1,24	1,38	1,41	-	1,53	-
3,5	1,30	1,47	1,50	-	1,62	-
4	1,37	1,55	1,59	-	1,70	-
4,5	1,43	1,64	1,68	-	1,77	-
5	1,49	1,73	1,76	-	1,85	1,51
10	2,11	2,58	2,63	-	2,47	2,11
15	2,76	3,44	3,50	-	-	2,89
20	3,41	4,32	4,39	-	-	3,66
25	4,08	5,21	5,30	-	-	4,44
30	4,77	6,11	6,21	-	-	5,21
35	5,46	7,03	7,14	-	-	5,99
40	6,16	7,96	8,08	-	-	6,76
45	6,87	8,89	9,03	-	-	7,54
50	7,59	9,84	9,99	-	-	8,31

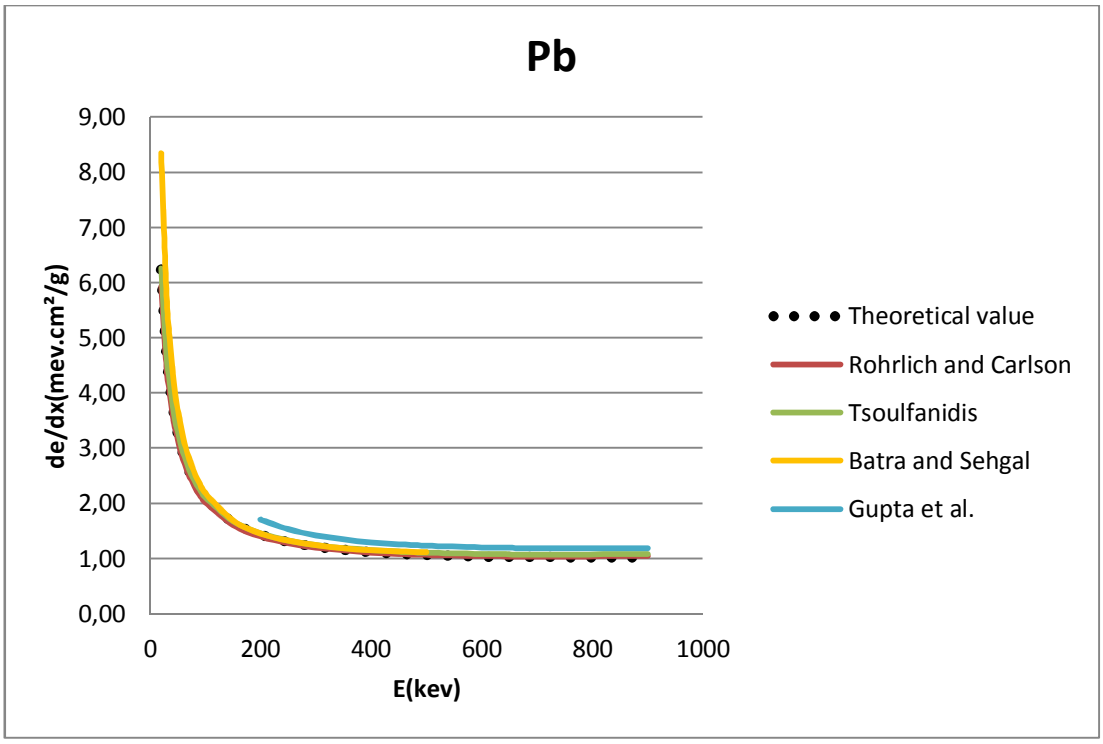

Figures 3.9 Stopping powers of positrons in Lead obtained by different methods of as a function of positron energy from 0 to 1 MeV.

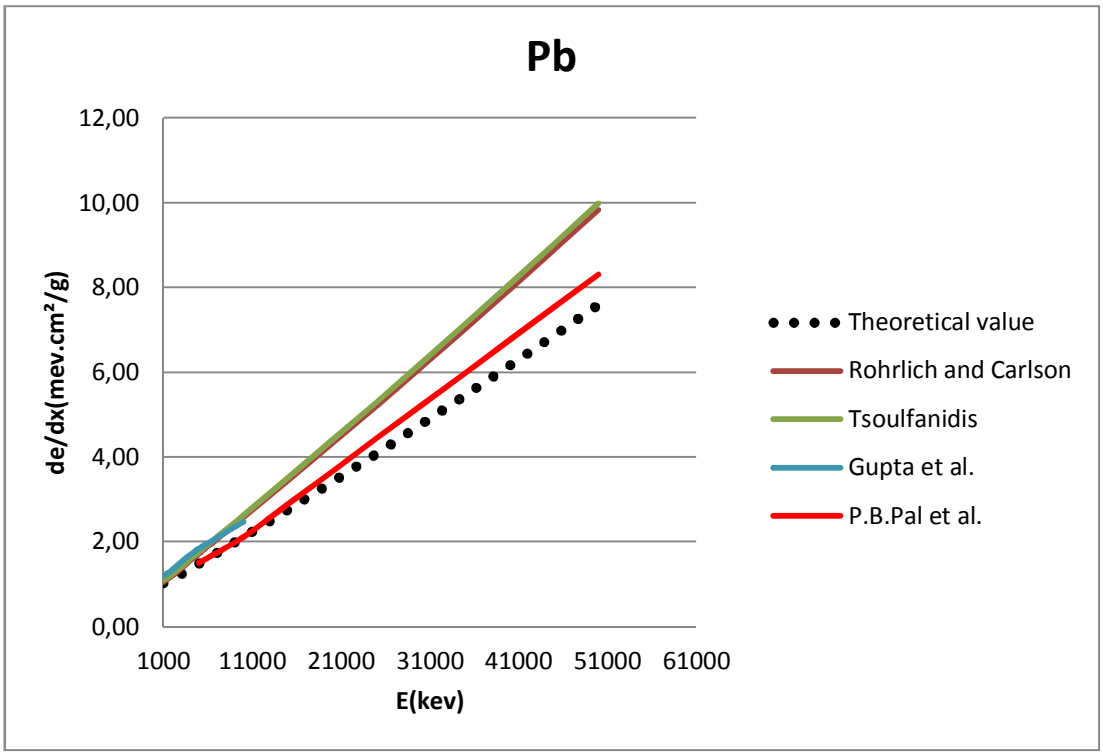

Figures 3.10 Stopping powers of positrons in Pb obtained by different methods of as a function of positron energy from 1 to 50 MeV.

CHAPTER 4

CONCLUSIONS

The knowledge of the features of the transmission and absorption of low, intermediate and high energy positron in elemental materials is of great importance for the experimental methods in nuclear and atomic physics. It is also useful in understanding the various interactions of these particles with matter.

The knowledge of the ranges of this particle in matter has useful applications for the study of biological effects, radiation damage dosage-rates and energy dissipation at various depths of an absorber. It has also useful applications in the design of detection systems, radiation technology, semi-conductor detectors and shielding by choosing the proper thickness of the target and especially in positron emission tomography (PET).

In this work, the stopping power of the positron in Al, Si, Ag, Cu, and Pb elements were determined by using five different methods. It is difficult to obtain the exact result of stopping power for the positrons. Hence many attempts have been done by the researchers to obtain empirical formulations to estimate the stopping powers of the positron in the elements. It was found that each method provides a proper result depending on the the energy range of the positron

Our calculations showed that Rohrlich and Carlson and Tsoulfanidis equations give better results with compared to the theoretical values at low energies up to 1.0 MeV. It is also observed that Gupta et al. method provides closer results to the theoretical results between 1.0 MeV to 10 MeV, while P. B. Pal et al. method gives better results from 5 MeV to 50 MeV. These observations are true for all investigated materials.

References

[1] P. A. M. Dirac. (1928). The Quantum Theory of the Electron, *The Royal Society,* **117**, 610–624.

[2] P. A. M. Dirac. (1929). A Theory of Electrons and Protons, *The Royal Society,* **126**, 360–365.

[3] F. Close. (2009). Antimatter, *Oxford University Press,* Oxford.

[4] P. A. M. Dirac. (1931). Quantised Singularities in the Quantum Field, *The Royal Society,* **133**, 60-72.

[5] F. Close. (2009). Antimatter, *Oxford University Press,* Oxford.

[6] J. Mehra, H.Rechenberg. (2000). The Historical Development of Quantum Theory, *Springer,* New York.

[7] Carl. D. Anderson. (1933). The Positive Electron, *Physical Review,* **43**, 491-494.

[8] R. D. Evans. (1955). The Atomic Nucleus, *McGraw-Hill,* New York.

[9] D. W. Rickey, R. Gordon, W. Huda. (1992). On Lifting the Inherent Limitations of Positron Emission Tomography by Using Magnetic Fields (MagPET), *Automedica,* **14**, 355-369.

[10] M. E. Phelps, J. C. Mazziotta, H. R. Schelbert. (1986). Positron Emission Tomography and Autoradiography , *Raven Press,* New York.

[11] H. E. Johns and J. R. Cunningham. (1983). The Physics of Radiology (fourth edition), *Charles C. Thomas,* USA.

[12] H. Bethe. (1930). Zur Theorie des Durchgangs schneller Korpuskularstrahlen durch Materie, *Ann. d. Physik,* **5**, 325.

[13] P. Sigmund. (2006). Particle Radiation and Radiation Effects, *Springer,* Berlin.

[14] R. K. Batra, M. L. Sehgal. (1970). Emprical Relation for Total Stopping Power of Positrons and Electrons, *Nuclear Physics,* **A156**, 314-320.

[15] S. K. Gupta, J. C. Govil, D. K. Gupta, R. K. Tyagi, O. P. Varma. (1982). Emprical Equations for the Stopping Power and C. S. D. A. Range Difference of 0.2 to 10 MeV Positrons, *Int. J. Appl.Radiat. Isot. ,* **33**, 773-774.

[16] N. Tsoulfanidis, S. Landsberger. (2010). Measurement and Detection of Radiation, *Crc Press,* New York.

[17] F. Rohrlich, B. C. Carlson. (1954). Positron-Electron Differences in Energy Loss and Multiple Scattering, *Physical Review,* **93**, 38-44.

[18] P. B. Pal, V. P. Varshney, D. K. Gupta. (1986). Total Stopping Power Formulae for High Energy Electrons and Positrons, *Nuclear Instruments and Methods in Physics Research,* **B16**, 1-4.